PHYSICAL MODELING OF DIESEL GENERATOR EXHAUST DISPERSION

LIMERICK GENERATING STATION UNIT 1 AND 2
PHILADELPHIA ELECTRIC COMPANY

by

M. Poreh,[1] W. W. Li,[2] J. E. Cermak,[3] and J. A. Peterka[3]

FLUID MECHANICS AND
WIND ENGINEERING PROGRAM

COLLEGE OF ENGINEERING

COLORADO STATE UNIVERSITY
FORT COLLINS, COLORADO

PHYSICAL MODELING OF DIESEL GENERATOR
EXHAUST DISPERSION

LIMERICK GENERATING STATION UNIT 1 AND 2
PHILADELPHIA ELECTRIC COMPANY

by

M. Poreh,[1] W. W. Li,[2] J. E. Cermak,[3] and
J. A. Peterka[3]

Fluid Mechanics and Wind Engineering Program
Fluid Dynamics and Diffusion Laboratory
Department of Civil Engineering
Colorado State University
Fort Collins, CO 80523

CSU Project 2-96170

February 1985

CER84-85MP-WWL-JEC-JAP42

---

[1]Visiting Professor, Wind Engineering Scholar for 1985, Colorado State University
[2]Research Associate, Colorado State University
[3]Professor, Fluid Mechanics and Wind Engineering Program, Colorado State University

ABSTRACT

Dispersion of exhaust gases from the Diesel Generating Units in the Limerick Generating Station was simulated in the Environmental Wind Tunnel at Colorado State University, using a 1:110 scale model and the concentration levels and excess temperatures at the various air intakes were predicted for different wind directions and stack configurations. The maximum concentrations were found to occur at the air intakes of reactor enclosure buildings.

The study shows that it is advantageous to eliminate the bend at the top of the present 7.5-ft stacks and exhaust the gases vertically, in order to reduce the concentration levels at the air intakes of the Reactor Enclosure Building.

The maximum concentration levels at the various air intakes are shown to decrease with the height of the stacks and increase with the wind speed. For example, the dilution of the exhaust gases from 46 ft stacks was below 1/425 for southern wind speeds above 15 mph, whereas similar dilution of exhaust gases from 27.5-ft stacks occurred at southern wind speeds above 12 mph. The yearly probability of exceeding these wind speeds has been estimated, but it is recommended that the final choice of the stacks height be made after examining the possibility of establishing testing schedules for the diesel generators that will take advantage of low winds at the site.

The maximum excess temperature at the Diesel Generator air intakes, was found to be 1°F, for the case of 2.5-ft stacks and high wind speeds from wind direction 292°.

TABLE OF CONTENTS

LIST OF TABLES

LIST OF FIGURES

LIST OF SYMBOLS

$( )_I$	at idling condition
WD	wind direction
$( )_F$	at full load condition
$( )_p$	value for prototype
$( )_m$	value for model
R_x	the scale for modeling any variable x; $R_x = x_m/x_p$ (see Table 2)
R(x)	identical to R_x
L	length scale
d	stack diameter (ID)
ρ	specific density
$( )_a$	value of ambient atmosphere
$( )_s$	value at stack
V_s	stack exit velocity
U	mean wind speed
U_a	mean ambient wind speed
U_R	mean reference wind speed (see p. 13)
$\Delta\rho$	$\rho_a - \rho_s$
ρ_a	ambient air density
ρ_s	density of exit gases
g	gravitational acceleration
T	absolute temperatures (°K)
c_p	specific heat at constant pressure
C	concentration per unit volume
C^m	concentration per unit mass
C_s	concentration per unit volume at the stack

A area in Equation (20)

q_m mass flux in Equation (20)

$(\ )_{pI}$ for prototype idling condition

$(\ )_{pF}$ for prototype full-load condition

$(\ )_{mI}$ for model idling condition

$(\ )_{mF}$ for model full-load condition

n power in Equation (33)

z height above ground

z_R reference height

Q discharge through air intakes

NOTATION OF BUILDINGS AND LOCATIONS (see Figures 1 and 8)

RAD Radwaste Building

TBW Turbine Building West

TBE Turbine Building East

CR Control Room

RBW Reactor Enclosure Building West

RBE Reactor Enclosure Building East

ADM Administration Building

DGW Diesel Generator Unit 1 (West)

DGE Diesel Generator Unit 2 (East)

1. INTRODUCTION

The Limerick Generating Station (LGS) is built on a flat hill approximately 1000 ft east of the Schuylkill River Valley. The general configuration of the LGS is shown schematically in Figure 1. It is composed of six major adjacent buildings: A 194-ft high Reactor Building (RB), a 105-ft high Turbine Building (TB) north of the RB, an Administration Building (ADM), a Shop Warehouse, and two 29-ft high Diesel Generating Buildings (DGB) south of the RB. At present only the western building (DGBW), which encloses Unit 1 Diesel Generators, is built and the area reserved for the DGBE (Unit 2) is vacant.

Each Diesel Generating Unit has four diesel generators which exhaust their gases through four 30-in. ID stacks near the southern edge of the building. The present configuration of the stacks is also shown schematically in Figure 1.

Exhaust concentrations at the various HVAC air intakes of the buildings are determined by local wind speed and wind direction, the configuration and height of the stacks, and by the initial characteristics of the plumes at the exit from the stacks.

The purpose of this study is to estimate the local concentrations of the exhaust gases and the local temperature rise at different air intakes for different ambient wind speeds and wind directions; and for several stack configurations; in order to identify an exhaust-system configuration which will result in acceptable concentrations and temperatures at the air intakes of the various buildings.

This was accomplished through physical modeling in the Environmental Wind Tunnel (EWT) at Colorado State University, using a physical model of the Limerick Generating Station (the prototype). The geometric scale of the model was 1:110. The model testing was divided into two parts:

(1) A flow visualization study aimed at identifying critical wind speeds and wind directions, and observing the complex flow pattern around the station. The highlights of the flow visualization study have been recorded on videotape and on black-and-white photographs.

(2) Measurements of concentration levels at various air intakes of the model, for different configurations and wind conditions, from which the dilution of the prototype concentrations and excess temperatures were calculated.

The report discusses the criteria necessary for simulating the plumes transport and diffusion, the selection of the model scales, the experimental methods and procedures, the testing program and the results of the measurements. The measurements are then analyzed and recommendations are made for reducing the concentration level at the various air intakes.

2. SIMILARITY REQUIREMENTS AND SELECTION OF MODEL SCALES

2.1 Background

One of the objectives of this study is to determine concentrations and excess temperatures near various air intakes, at critical wind speeds at which the plumes impact near these intakes. It was impossible to predict the values of these critical wind speeds and they have been therefore determined during the initial visualization phase of the study. A very rough estimate had indicated, however, that these speeds, and the corresponding Reynolds numbers, could be relatively small, particularly for the case of idling, at which both the buoyancy flux and the momentum flux of the plumes are small. It was therefore decided to increase, as much as possible, the wind speeds in the model by using a large geometric scale

$$R_L = \frac{L_m}{L_p} = \frac{1}{110}$$

The blockage in the wind tunnel at this scale is less than 10 percent, the allowed blockage for wind tunnels with adjustable ceilings. A further increase of the model velocities has been achieved by using a slightly larger scale for the stack diameter

$$R_d = \frac{d_m}{d_p} = \frac{1}{80}$$

The 38 percent distortion of the stack diameter (110/80) can hardly affect the concentrations in the far field, which are primarily determined by the buoyancy flux and momentum flux (Poreh et al., 1981), but makes it possible to increase the Reynolds numbers in the model. It should be stressed that high model Reynolds numbers are essential for a correct simulation of the turbulent nature of the flow (Poreh et al., 1981).

2.2 Similarity Requirements

As shown by Poreh et al. (1981), it is required that the ratio of the dimensionless buoyancy flux in the model and prototype be 1, or

$$R \frac{\Delta\rho g V_s d^2}{\rho_a U_a^3 L} = \frac{\left(\dfrac{\Delta\rho g V_s d^2}{\rho_a U_a^3 L}\right)_m}{\left(\dfrac{\Delta\rho g V_s d^2}{\rho_a U_a^3 L}\right)_p} = 1 \qquad (1)$$

and, similarly the ratio of the dimensionless momentum flux in the model and prototype be 1, or

$$R \left(\frac{\rho_s \; V_s^{\,2} \; d^2}{\rho_a \; U_a^{\,2} \; L^2}\right) = 1 \qquad (2)$$

where R_x or $R(x)$ is defined as the ratio x_m/x_p of any variable x in the model (x_m) and prototype (x_p), respectively, as shown in Equation (1) above.

It is also desired that:

$$R \left(\frac{V_s}{U_a}\right) = \frac{R(V_s)}{R(U_a)} = 1 \pm 0.2 \qquad (3)$$

and

$$R \left(\frac{d}{L}\right) = \frac{R_d}{R} = 1 \pm 0.4 \qquad (4)$$

to avoid a large distortion of the exit conditions. The density ratios in the model and prototype will be adjusted to satisfy Equations (1) and (2).

2.3 Prototype Data

Stack diameter (d_p) = 30" = 0.762 m. Ambient temperature (T_a) = 308°K (95°F).

At full-load condition:

$$V_s = 30.3 \text{ m/sec}$$

$$T_s = 672°K \ (750°F)$$

$$\frac{\rho_s}{\rho_a} = \frac{T_a}{T_s} = 0.458$$

$$\frac{\Delta\rho}{\rho_a} = \frac{T_s - T_a}{T_s} = 0.542$$

The Froude number is defined here as $Fr = \rho_a V_s^2/(\Delta\rho \ g \ d) = 227.$

At idling condition:

$$V_s = 8 \text{ m/sec}$$

$$T_s = 477°K \ (400°F)$$

$$\frac{\rho_s}{\rho_a} = 0.646$$

$$\frac{\Delta\rho}{\rho_a} = 0.354$$

$$Fr = 24.$$

2.4 Simulation of Full-Load Conditions

We have selected for the simulation of the full-load conditions the velocity ratio scale

$$R\left(\frac{V_s}{U_a}\right) = 1 \tag{5}$$

It follows from Equation (2) that

$$R\left(\frac{\rho_s}{\rho_a}\right) = \frac{R_L^{\ 2}}{R_d^{\ 2}} = \left(\frac{80}{110}\right)^2 = 0.529 \tag{6}$$

Thus, the density ratio in the model should be

$$\left(\frac{\rho_s}{\rho_a}\right)_m = 0.529 \text{ x } 0.458 = 0.242 \tag{7}$$

$$\left(\frac{\Delta\rho}{\rho_a}\right)_m = 0.758 \tag{8}$$

and

$$R\left(\frac{\Delta\rho}{\rho_a}\right) = 1.398 \tag{9}$$

To satisfy Equation (1) it is necessary that

$$R(U_a) = R(V_s) = \left(\frac{R(\Delta\rho/\rho_a)\ R_d^{\,2}}{R_L}\right)^{1/2} = \frac{1}{6.45} \tag{10}$$

One sees that the 38 percent distortion of the stack diameter in the model has made it possible to increase the wind speed in the model by 63 percent ($\sqrt{110}/6.45$).

2.5 Simulation of Idling Conditions

The present model includes a simulation of air flow through the major air intakes and exhausts of the building. The discharge of the air, during the full-load tests, has to be scaled as

$$R_{QAC} = R(U_a)\ R_L^{\,2} = \frac{1}{78045}$$

It is of great advantage to use the same discharge scale during the modeling of the idling operation. To achieve this we shall therefore select the same $R(U_a)$ for all the full-load and the idling tests.

$$R(U_a) = \frac{1}{6.45}$$

It will also be convenient to use in these tests the same stack diameter scale and geometric scales

$$R_d = \frac{1}{80}\ ;\quad R_L = \frac{1}{110}$$

To satisfy the model criteria (Equations (1) and (2)), it is required that during the modeling of idling conditions

$$R\left(\frac{\Delta\rho}{\rho_a}\right) \cdot R(V_s) = \frac{R(U_a)^3 \, R_L}{R_d^{\,2}} = \frac{1}{4.612} \tag{11}$$

$$R\left(\frac{\rho_s}{\rho_a}\right) \cdot R(V_s^{\,2}) = \frac{R(U_a)^2 \, R_L^{\,2}}{R_d^{\,2}} = \frac{1}{78.65} \tag{12}$$

Since $(\Delta\rho/\rho_a)_p = 0.354$ and $(\rho_s/\rho_a)_p = 1 - \Delta\rho/\rho_a = 0.646$, it follows that

$$\left(\frac{\rho_s}{\rho_a}\right)_m R(V_s^{\,2}) = \frac{1}{121.8} \tag{13}$$

and

$$\left[1 - \left(\frac{\rho_s}{\rho_a}\right)_m\right] R(V_s) = \frac{1}{13.03} \tag{14}$$

The solution of these equations gives

$$\left(\frac{\rho_s}{\rho_a}\right)_m = 0.439 \tag{15}$$

and

$$\left(\frac{\Delta\rho}{\rho_a}\right)_m = 0.561 \quad , \tag{16}$$

as well as a new scale for the exit velocity of the plume during idling conditions:

$$R(V_s)_I = \frac{1}{7.31} \quad , \tag{17}$$

which corresponds to $R(U_a/V_s)_I = 1.13$, a very small (13 percent) distortion of the exit velocity.

The scale of the density ratio in the idling case should thus be:

$$R\left(\frac{\rho_s}{\rho_a}\right) = \frac{0.439}{0.646} = \frac{1}{1.471} \tag{18}$$

$$R\left(\frac{\Delta\rho}{\rho_a}\right) = 1.585 \tag{19}$$

2.6 Concentrations, Excess Temperatures and Dilution Rates

One should distinguish between concentrations per unit volume, C, and concentrations per unit mass C^m. All the data in this report are of concentrations per unit volume (expressed in ppm).

According to the mass conservation equation, the distribution of the concentration of any pollutant across a plume satisfies the equation:

$$\int_A \rho\, c^m\, u\, dA = q_m \tag{20}$$

where $q_m = \rho_s C_s^m V_s A_s$ is the mass flux from the stacks,

ρ = the local density, and

u = the local velocity.

Our measurements will be made at relatively large distances from the stacks (distances larger than 10 stack diameters), where the velocity field and the dimensionless concentration distributions are determined by the dimensionless momentum flux and the dimensionless buoyancy flux at the source. Moreover, the air density at such distances is close to the ambient air density ρ_a. It follows from dimensional considerations that the dimensionless concentration at each point $\rho_a U_a L^2 C^m/q_m$ is a function of the dimensionless momentum flux and dimensionless buoyancy flux at the source. Since the physical simulation is performed so that these dimensionless independent variables are the same in the model and prototype, it follows that the dimensionless concentrations are also equal in the model and prototype, or:

$$R\left(\frac{\rho_a U_a L^2 C^m}{\rho_s V_s A_s C_s^m}\right) = 1 \tag{21}$$

The concentration per unit volume C is related to the concentration per unit mass by

$$C = \rho C^m \quad . \tag{22}$$

Thus,

$$R\left(\frac{CU_a L^2}{C_s V_s A_s}\right) = 1 \tag{23}$$

The model scale for the concentration ratio C/C_s is thus

$$R(\frac{C}{C_s}) = R(\frac{V_s}{U_a}) \cdot R_d^2/R_L^2 \tag{24}$$

and

$$\left.\frac{C}{C_s}\right|_p = \left.\frac{C}{C_s}\right|_m \cdot \frac{1}{R(C/C_s)} \tag{25}$$

Using the previously calculated scales, one finds that for full-load operations

$$R(C/C_s)_F = 1.89 \tag{26}$$

and for idling

$$R(C/C_s)_I = 1.67 \tag{27}$$

The temperature field satisfies the energy conservation equation

$$\int_A \rho c_p(T-T_a)udA = \rho_s c_p(T_s-T_a)V_s A_s \tag{28}$$

It is reasonable to assume that at high Reynolds numbers the excess temperature will be distributed as the concentration per unit mass C_m, as $c_p T$ is the energy per unit mass. It follows from dimensional considerations that

$$\frac{\rho_a c_p(T-T_a)U_a L^2}{\rho_s c_p(T_s-T_a)V_s A_s} = \frac{\rho_a C^m U_a L^2}{\rho_s C_s^m V_s A_s} \tag{29}$$

or

$$\frac{T-T_a}{T_s-T_a} = \frac{C^m}{C_s^m} = \frac{\rho_s}{\rho_a}\frac{C}{C_s} \tag{30}$$

Thus, the dilution of the excess temperature in the prototype, for full-load operations, is given by

$$\left.\frac{T-T_a}{T_s-T_a}\right|_{pF} = 0.46 \left.\frac{C}{C_s}\right|_{pF} \tag{31}$$

Similarly, for idling:

$$\left.\frac{T - T_a}{T_s - T_a}\right|_{pI} = 0.65 \left.\frac{C}{C_s}\right|_{pI} \tag{32}$$

The final values of the scale factors for the different variables are listed in Table 1.

3. EXPERIMENTAL METHODS AND PROCEDURES

3.1 General

A 1:110 scale model of the LGS and surrounding buildings was constructed. The inner diameter of the stacks was determined, however, using a 1:80 scale, as explained on page 3. Figure 2 shows photographs of the model installed in the Environmental Wind Tunnel (EWT) from different directions. The model was centered on the 12-ft turntable of the EWT so that the wind direction can be changed easily.

Eight spires were installed at the entrance to the test section (see Figure 2) to produce the desired approach velocity distribution.

The diesel exhaust gases in the model contained 2% ethane. The concentrations of the ethane at various air intakes were determined, using gas chromatography techniques, for different wind directions, speeds and stack configurations. Visualization of the plumes was achieved by adding titanium tetrachloride (TTC) smoke to the exhaust gases. A detailed description of the experimental techniques follows.

3.2 The Environmental Wind Tunnel, the Scale Model, and the Approach Velocity Profile

The Environmental Wind Tunnel (EWT) is shown in Figure 3. The model was located on the center of the 12-ft turntable. The cross-section of the wind tunnel upstream of the model was 12 ft x 6 ft. The ceiling above the model was raised to h = 6.6 ft in order to obtain a zero pressure gradient along the tunnel and thus reduce the blockage effect caused by the large model. The blockage of the tunnel was around 10%, and thus falls within the allowable blockage range for wind tunnels with adjustable ceilings [EPA, 1979; see References].

Eight 6-ft spires and a 7-in. barrier were installed at the entrance to the test section, as shown in Figure 2. No artificial roughness was added downstream of the spires in order to produce the velocity profile and turbulence distribution upstream of the model shown in Figures 4 and 5.

This particular configuration was chosen for the following reasons. The location of the stacks suggests that the highest concentrations at the air intakes will occur at southern winds. The concentration fields for easterly and westerly winds were expected to be small, irrespective of the approach velocity profile. The concentration field for northern winds is primarily determined by the wake of the building and is thus expected to be small and practically independent of the approach velocity profile. It was therefore decided to use one approach velocity profile for all tests, which will simulate, as much as possible, the estimated velocity profile for steady-state, continuous southern winds.

No field measurements of the approach velocity profile are available, and there was no way to include in the model, at the required scale, the Schuylkill Valley located to the west and southwest of the station. It is estimated, however, that the presence of the hill would flatten out the southern approach velocity profile. A similar effect is obtained by a rough-to-smooth transition of the terrain and it was therefore decided to leave the wind tunnel floor between the spires and the model as smooth as possible.

The approach mean velocity and turbulence profiles of upstream the LGS model were measured with a Thermo System hot-wire probe and are shown in Table 2 and Figure 4. The approach velocity profile is also plotted in Figure 5 using log-log coordinates, which shows power laws such as

$$u(z)/U_R = (z/z_R)^n \tag{33}$$

as straight lines. One sees from Figure 5 that the upper section of the velocity profile is characterized by a power $n \cong 0.25$, whereas the lower part has a flatter velocity profile, $n \cong 0.1$, as desired.

The reference wind-tunnel speed U_R was monitored during the tests using a calibrated Datametric Velocity Probe, placed at the height of 55 in. (140 cm) above the floor (prototype EL 504 ft). <u>When referring to wind speed in the report, we shall always refer to this reference velocity expressed in prototype values</u>.

Most of the meteorological data, and in particular the probability distribution of the wind in the region reproduced in Table 2 are based on measurements at the height of 30 ft (EL 280) and 270 ft (EL 520) at Meteorological Tower #1; which is built on a hill (EL 250) north of LGS. It is interesting to note that the mean wind speed at 270 ft is approximately 1.8 times larger than the wind speed at 30 ft. Using Figure 7 we have estimated that the ratio of high southern wind speeds at the two heights is approximately 1.66 which corresponds to $n = 0.23$ in Equation (33).

In order to estimate probabilities of occurrence of given concentration values at the various air intakes at LGS, one should estimate the probabilities of U_R. Since U_R is measured at almost the same elevation as the 270 ft data at the Meteorological Tower, it will be assumed that the probability distribution in Table 3b is identical to that of U_R.

A better estimate of the correlation between the two data sets can be obtained, if necessary, by simulating the flow over the entire region using a smaller wind-tunnel model.

3.3 Selection of Stack Exhaust Gas

For simulating full load conditions we have selected a mixture of

CH_4 (mw = 16) - 2.0%

He (mw = 4) - 86.5%

N_2 (mw = 28) - 11.5%

The combined density ratio would be

$$\frac{\rho_s}{\rho_a} = \frac{0.02 \times 16 + 0.865 \times 4 + 0.115 \times 28}{28.96} = 0.242$$

For simulating idling condition we have selected a mixture of

CH_4 - 2.0%

He - 62.7%

N_2 - 35.3%

which gives

$$\rho_s/\rho_a = 0.439$$

It is often found that certified gases prepared by manufacturers have slightly different densities from that specified in the order. If the deviation of ρ_s/ρ_a from the required value is of only a few percent, the effect on the simulation is rather small. Note, for example, that the plume rise is proportional to the buoyancy flux to the 1/3 power.

3.4 Intakes and Exhausts Air Flows

The high-volume ventilation system is simulated in the tests at a scale of

$$R_{QAC} = R_L^2\ R(V_a) = 1/78045 \tag{34}$$

The simulated air flows in the prototype and in the model are specified below:

Location	Q_p (cfm)	Q_m (lit/min)
Diesel Generating Build. (Unit 1 or Unit 2). Full load value:	204000	74
Radwaste Building:	78300	29
Reactor Building:	2x234000	2x85
Turbine Building:	2x250000	2x91

The south stack of the reactor building exhausts the air which enters the building through the two intakes of that building. The north stack exhausts the air from the Turbine and Radwaste Buildings. The discharge of the air from the exhaust ducts of the Diesel Generating Unit was assumed in the simulation to be equal to the discharge which enters the building through the intakes, although in the prototype it is slightly smaller, due to the configuration of the combustion air intake port.

It should be noted that although the flow rates into the buildings are relatively large, their effect on the air flow around the buildings is not expected to be very large, as these flow rates are only a few percent of the volume of air which approaches the building and has to go around it. (Approximately the air speed times the area of the buildings.)

The air flow through the various intakes and exhausts in the model was produced by an air pump operated by a DC motor, as shown schematically in Figure 6. The discharge through the 11 inlets and outlets of the pump is proportional to the adjustable pressure in the chamber and the area of each orifice, as this pressure is primarily lost in the orifice. The air flow through the pump, as a function of the gage pressure in the air pump, upstream of the fan was determined. During the tests the pressure at that point was monitored using a pressure transducer. The pressure loss through the pipes connecting the air pump to the various inlets and exhausts in the model is estimated to be of the order of 4 percent of the losses at each orifice.

The external pressure on the building at the critical wind speeds is expected to be of the order of 1.5 mm H_2O for the simulation of full-load conditions and much smaller for the simulation of idling conditions, and its effect on the discharge through any of the inlets or exhausts is estimated to be smaller than 5 percent.

3.5 Concentration Measurements

The test procedure consisted of the following steps: (1) setting the desired tunnel-wind speed, (2) operating the air pump for the simulation of the HVAC system, (3) setting the desired discharge of the source gas from the stacks. (4) After the flow had been established, withdrawing samples of air from the locations of the air intakes. (5) The air samples are then injected one by one into the gas chromatograph which measures the volume concentration of the ethane in each sample.

Samples were taken of the ambient concentration upstream of the model at each run. The concentrations given in this report are the concentrations per unit volume, in ppm, above the background concentration.

The dilution rate in the model was calculated by the ratio of the measured concentration to the source concentration (20,000 ppm). We shall refer in the report only to the prototype values of the concentration ratio $(C/C_s)_p$, calculated using Equations (24)-(27). Since this ratio is usually small, we shall present in the report the value of 10,000 C/C_s.

3.6 Quality Control Procedures

To ensure quality control of the experimental work and analysis, the following experimental procedures were adopted:

(1) Certified gas mixtures were supplied by Scientific Gas Products, Inc., Longmont, Colorado, with certification of ±2% accuracy. The concentrations of ethane in the source gas were also checked by the gas chromatograph, Hewlett-Packard Model 5700A Flame Ionization Gas Chromatograph, used in analyzing the concentrations at the various air intakes.

(2) The gas chromatograph can measure samples with sensitivity down to picogram (10^{-12}) levels. It was calibrated with a certified ethane mixture (Scientific Gas Products, Inc., Longmont, Colorado) of 2010 ppm, at least four times a day, before and after concentration measurements. The maximum error expected from the gas chromatograph was found to be less than 1.0 percent from the mean based on 10 observations.

(2) A Fisher-Porter (F-P) medium flow rator was employed to yield a desired flow rate of the exhaust gases. A pressure gauge and a needle valve were installed between the stacks and the flow rator so that back-pressures were kept constant. The flow rator was first calibrated against a bubble flow meter and later against a Matheson Linear Mass Flow Meter, with same source gases. The mass flowmeter was used to monitor flow rates in addition to the F-P flow rator.

(4) Measurements of mean velocity and turbulence intensity profiles were obtained with a TSI Model 1053B constant-temperature anemometer in conjunction with Model 1210-20 Platinum Hot Film. Calibration of the hot-film probe was performed using a Matheson Linear Flow Meter and Controller. A Model 1800 LV Datametric Linear Flow meter and Probe was used to monitor the reference wind speed. An HP-2401 Integrating Digital Voltmeter was used to determine the Datametrics reading by integrating the signal over a 100-second interval.

(5) The pressure transducers (Statham Model PM 283TC) had been calibrated using transducers with traceable standards.

(6) All records have been checked daily by supervising personnel.

4. THE EXPERIMENTAL PROGRAM

4.1 Flow Visualization

The purpose of the flow visualization phase was to visually assess the structure of the flow near the LGS and to observe the plumes released from different stack configurations and their possible impact on the buildings near the various air intakes at different wind directions and speeds.

Preliminary analysis had indicated that the plumes would rise above the Reactor Building (RB) at low wind speeds, but will impact on the RB at high speeds. It was therefore decided to record the plume behavior at two wind speeds. A relatively low wind speed of U_R = 8 mph (U_R is the reference velocity expressed in prototype values) and 12 or 16 mph. The probabilities of encountering <u>southern</u> wind speeds, which are higher than the above speeds are estimated from Table 3b and Figure 7, to be of the order of 55 percent, 24 percent and 8 percent. The overall probability of encountering southern winds is 7.23 percent. The probability of encountering high eastern winds appears to be slightly lower, whereas the probability of encountering high wind speeds from the west, and particularly from WD = 292°, is much higher. Thus, flow visualizations for critical western directions were recorded at reference speeds of 16 mph.

Twenty-eight runs were recorded on videotape, see Table 4. A series of still photographs was also taken at the same configurations. The still photographs were made using 4 sec exposures, so that only the average plume positions can be seen in these photographs.

4.2 The Concentration Measurement Program

The flow visualization program made it possible to draw the following conclusions:

(a) The most critical wind direction is WD = 180°.

(b) Plumes from Unit 2 do not impinge on the building in westerly winds. In easterly winds, the plumes from Unit 2 behave in exactly the same way as plumes from Unit 1 at symmetrical wind directions with respect to the south. (For example, Unit 2 at WD = 60° will behave as Unit 1 at WD = 300°).

(c) The concentrations usually increase with the wind speeds.

In view of these conclusions and since the probability of high wind speeds from easterly wind directions is considerably lower than the probability of such winds from symmetrical westerly wind directions, it was decided to focus the concentration measurements on the case of Unit 1 operating at wind directions 180°-360° and to increase the number of sampling points beyond the original plan, in order to obtain a better picture of the concentration field.

The location of various sampling tubes and their notations are specified in Figure 8. Note that the sampling tubes RBW1, RBW2, RBE1, and RBE2 were located inside suction tubes which simulated the HVAC system at these air intakes.

The concentration measurement program is specified in Table 5. The table also points out the air intakes where measured concentration ratios were above critical values, which will be specified in the following chapter.

The results of the various runs are shown in Table 6, where the runs appear according to their position in Table 5. The table also contains the calculated prototype concentration ratios C/C_s, multiplied by 10,000, at the various locations. Note that all concentrations given in this report are the measured concentration of the tracer in the model above the background concentration of that tracer in the upstream wind, and that the source concentration was always 20,000 ppm.

5. ANALYSIS OF THE EXPERIMENTAL RESULTS

5.1 The Flow Visualization Program

The flow visualization program clearly confirmed the intuitive assessment that the most critical wind direction, at which high concentrations at the Reactor Building Air Intakes (RBW and RBE) would occur, is WD = 180°.

It was observed in the tests that a coherent eddy is established at this wind direction above the Diesel Generating Buildings. One can recognize the swirling motion of this eddy in Figure 18.* Numerous runs at this wind direction established the beneficial effects on the concentration at the air intakes of the following parameters:

(a) A vertically directed exit of the gases from the stacks, compared to the original horizontal exit toward the building (see Figures 9 and 10). Early tests with an inclined exit of gases toward the south did not establish a clear beneficial effect of such an inclination and the study has therefore continued with simple vertical stacks.

(b) The Height of the Stacks. When the stacks were sufficiently high, the plumes penetrated through the existing eddy and were not carried toward the air intakes. Figures 10-16 clearly show the effect of the stacks' height.

It was clear from the visualization tests that the plume from a 46-ft stack rises above the air intake RBW at wind speeds $U_R < 12$ mph (Figures 15 and 16). At $U_R = 16$ mph (Figure 17), however, increased concentrations at the air intakes can be expected.

---

*The reader is encouraged to view the video recordings of the flow visualization.

Figure 14 shows that the critical wind speed for the 27.5-ft stacks operating at full load would be lower, around 12 mph.

(c) Higher momentum and buoyancy fluxes at the exit. Increasing these fluxes is equivalent to an increase of the stacks' height. At many wind speeds, plumes from the diesel generators operating at full-load (high fluxes) can penetrate the existing eddy and rise above the air intakes, but when the load is reduced (idling) the plume is partially trapped in the eddy and impinges at the air intakes. See, for example, Figures 18 and 19.

(d) Operation at low wind speeds. Local velocities and the rotational speed of the close-by eddy increase with the wind speed, and the high wind speeds reduce the plume rise and increase the concentrations at the air intakes.

The flow visualization tests also showed that high concentrations might occur at additional wind directions:

(1) WD = 202.5°, at which the plumes from Unit 1 are transported toward the air intake at the Eastern Reactor Building (RBE).

(2) WD = 247° and 292°, at which the plumes pass close to the Administration Building (ADM) (see Figures 21 and 22). One can also see in these figures that the edges of the plume reach intermittently the eastern section of the Diesel Generator Air Intake Unit 2, and it was therefore decided to have two sampling tubes at that location (DGE1 and DGE2), as shown in Figure 8.

(4) WD = 360°. At this wind direction no direct impact of the plume at the locations of the air intakes was observed, but part of the plume was trapped in the wake of the building, suggesting that high concentrations in the entire wake region might occur. The video

recordings of this case, run 20, show that it took a long time for gases trapped in the wake to clear that region after the operation of the diesel generators was stopped.

The above critical wind directions were established at reference wind speeds between U_R = 12 to 16 mph, for plumes from the western Diesel Generating Unit - Unit 1. As mentioned earlier, plumes from Unit 2 did not come close to the air intakes at these westerly wind directions. At easterly wind directions, the behavior of the plumes from Unit 2 was found to be symmetrically similar to plumes from Unit 1 at westerly wind directions. Plumes from Unit 2 at WD = 60° behaved, for example, like plumes from Unit 1 at WD = 300°. However, the probability of high wind speeds from the east is much smaller (see Table 3b). For example, the yearly probability of U_T > 12.5 mph at WD = 67.5 is only 0.82 percent compared to a probability of 7.62 percent (9 times higher) at WS = 292.5°.

The visualization tests also did not show any effect of the Eastern Diesel Generator Building - Unit 2 on the large-scale flow structure and on the behavior of the plumes from Unit 1. It was therefore decided to include that building in the model only for tests with WD = 202° - 360°, at which concentrations at both DGE1 and 2 were expected to be significant. At WD = 180° an average value of C was measured at the place reserved for that building.

5.2 Analysis of the Concentration Measurements

5.2.1 Acceptable Dilution Rates

In order to evaluate quantitatively the significance of the measured concentration ratios and the calculated prototype concentration ratios, it is necessary to define what are the necessary dilution rates of the gases from the initial source concentration. We have used in the analysis the following criteria, proposed by the Bechtel Power Corporation (discussion with Mr. Jorge Schulz):

(1) At all air intakes except at the Control Room and the Administration Building, concentration ratios during any <u>one diesel generator operation</u> should satisfy the requirement

$$10{,}000\,\frac{C}{C_s} < \frac{10{,}000}{424} = 23.5 \text{ (for one operating generator)} \qquad (35)$$

Since we have tested in most runs the simultaneous operation of four stacks, the dilution rates in such runs may be four times larger, namely

$$10{,}000\,\frac{C}{C_s} < 94 \qquad (36)$$

(b) During an emergency, when the four stacks operate together, the concentrations at the Turbine, Reactor and Radwaste Buildings are allowed to be high, since the reactor intakes will be closed. However, it is required that concentrations at the air intakes of the Control Room (CR) satisfy the requirement

$$10{,}000\,\frac{C}{C_s} < 23.5 \quad \text{(CR and ADM for four operating generators)} \qquad (37)$$

(c) The required concentration ratios at the Diesel Generator Intakes should always be less than 1:100, even when the stacks of the four generators are broken (simulated by 2.5 ft stacks). Namely,

$$10{,}000\,\frac{C}{C_s} < 333 \quad \text{(DGW and DGE for four operating generators)} \qquad (38)$$

We have identified in Table 5 the locations at which the above criteria were not satisfied. Note that in Table 5d, we have used the criteria established for normal operation for all intakes, although the concentrations at the air intakes, except at ADM, CR, DGW and DGE, may be higher.

5.2.2 Concentrations at the Diesel Generators Air Intakes

In no test, including the tests of the 2.5 ft stacks, were the concentration ratios at DGW and DGE above the allowed values. The highest concentrations are expected to occur at high wind speeds from WD = 292° to WD = 315°, during the operation of 2.5 ft stacks. Runs 155, 163 and 164 show that the maximum ratios obtained at these cases were 10,000 $C/C_s \leq 33$, namely one-tenth of the allowed value according to Equation (38).

It was observed in the flow visualization tests that plumes from the high stacks are carried toward DGE (see Figure 21). Indeed, relatively high concentrations were measured at DGE at these cases [see Run 157 Table 6 (27)], but they were only one-fifth of the allowed concentrations.

It should be stressed, however, that the model tests with the 2.5 ft stacks simulated an unobstructed vertical exit of the gases from the stacks. Debris, which might partially cover the stack exits and deflect the plumes, could easily increase the concentration at the nearby air intakes of the diesel generators; however, it is understood that the cast iron construction of the stacks makes their blockage unlikely.

5.2.3 Concentrations in the Control Room and the Administration Building Air Intakes

At no run were the concentration ratios at the air intake of the control room above the maximum allowed values. Only at WD = 202° was a value of 10,000 $C/C_s = 20$ recorded at CR at a wind speed of 22.5 mph

[Run 126 Table 6 (21)]. However, the value dropped to 11 at a speed of 16 mph.

The values of C/C_s recorded at the Administration Building, during the operation of four 46-ft stacks, was only at two wind directions close to the maximum allowed value (10,000 C/C_s = 19 at WD = 300° and 10,000 C/C_s = 16 at WD = 202°). The reference wind speeds at these runs were around 21 mph. Once the wind speed was reduced to 16 mph, the concentration values decreased drastically [compare, for example, run 126 with run 127 in Table 6 (20 and 21)].

During the operation of the 2.5-ft stacks, however, the concentrations at the Administration Building have increased considerably. Figure 23 shows the maximum recorded values of C/C_s at ADM for this case, as a function of wind direction. The measurements were taken at U_R = 21 mph except where noted near the data point.

The critical wind directions for the Administration Building are WD = 202° and WD = 225°. However, even at these wind directions the excess concentrations were not very high and they dropped drastically with the wind speed.

5.2.4 Concentrations at the Reactor Building Air Intakes during Full-Load Operation

The highest concentration ratios at the RBW or RBE are expected to occur at high wind speeds. We have therefore tested the concentration ratios at reference speeds of approximately 21 mph. The values obtained at this wind speed should be regarded as the maximum values which can be obtained at these locations.

Figure 24 shows the predicted prototype concentration ratios at high wind speeds for 46-ft stacks and 27.5-ft stacks. The left-hand ordinate gives the concentration ratio for the operation of one diesel generator and the right-hand ordinate gives the concentration ratios for the operation of four diesel generators. The values shown in the graph are the maximum recorded values at any of the 10 sampling tubes of RBW and RBE.

Most of the values were measured during the simulation of four generators. At critical wind directions we have also included in the graph the maximum values recorded during the operation of the "worst" stack; No. 1 for westerly winds, No. 3 or 4 for southerly winds (see Figure 8).

It was surprising to find that the concentration ratio for the "worst" 46-ft stack at WD = 180° was approximately equal to one-fourth of the concentration ratio obtained during the simultaneous operation of the four 46-ft stacks, although the contributions of the individual stacks were not at all the same. In fact, the sum of the concentrations found during the operation of the four individual stacks was much lower than the concentration recorded during the simultaneous operation of the four stacks (see Figure 25 at wind speed 21.5). We have confirmed this result in a second series of runs and came to the conclusion that the simultaneous operation of the four stacks, which exhaust the gases at speeds of 65 mph, increased the rotational speed of the eddy formed near the base of the Reactor Building so that more exhaust gases were drawn in this case toward the Reactor Building (RBW) air intake. A milder similar effect was observed during the operation of the 27.5-ft stacks. In this case the "worst" stack gave a concentration value of only 20% higher than one-fourth of the value obtained when the four 27.5-ft stacks operated together.

The above concentration ratios were measured at relatively high speeds, which might never occur at these particular critical wind directions. In Figures 25 and 26 we have shown the dependence of the concentration ratio on the reference wind speed, U_R.

One clearly sees from Figure 25 that the concentration ratio for the 46-ft stacks drops below the critical value when $U_R \leqq 15$ mph. On the other hand, permissible concentration levels for the 27.5-ft stacks are obtained only when $U_R \leqq 12$ mph.

A similar situation exists for WD = 202°, where the critical wind speeds for 46-ft stacks and 27.5-ft stacks are approximately 16.5 mph and 14.5 mph, respectively. At WD = 225° the critical wind speed for the 27.5-ft stacks is 14.5 mph, whereas the concentration ratio for the 46-ft stacks approaches the critical values only at unrealistically high wind speeds.

Figure 27 shows the maximum concentration ratios measured at RBW for an idling diesel generator and 46-ft stacks. The measurements were made with four generators operating simultaneously. The wind direction is WD = 180°. The figure clearly indicates that only at reference wind speeds above 14.5 mph do the concentration ratios exceed the permissible value, but even at these wind speeds the excess concentrations were not very high. The concentration levels at other wind directions are expected to be lower than the permissible values.

It is estimated that the 27.5-ft stack would give higher concentration ratios (10,000 C/C_s of the order of 70) at reference wind speeds higher than 10 mph.

Concentrations at both RBW and RBE for four diesel generators and 2.5-ft stacks at medium and high wind speeds will be above the value allowed for normal operation, for all southerly wind speeds WD = 180°±60°, as shown in Figure 28. The maximum concentration ratio, recorded at WD = 180°, is 0.036 = 1/28!

5.2.5 Concentration Levels at the Turbine and Radwaste Buildings Air Intakes

Concentration levels at these air intakes always satisfied the requirement given in Equation (35).

5.3 Excess Temperatures

Excess temperatures above the ambient temperature can be calculated from the concentration ratios using Equations (31) and (32).

For full-load operation $T_S - T_a$ of the exit gases is 655°F. Thus the excess temperature would be

$$(T - T_a)°F = 655 \cdot 0.46 \cdot C/C_s = 301\ (C/C_s)_p = 0.03\ (10{,}000\ C/C_s)_p \qquad (39)$$

Using this equation the excess temperatures can be calculated directly from Table 6. The right-hand ordinate of Figure 28 gives the values of the excess temperatures for the operation of four 2.5-ft stacks. One sees that the maximum expected temperature rise, recorded at one location near RBW, is 11°F. We have also shown in that figure the average value of the concentration ratios and excess temperatures at both RBW and RBE. The maximum average temperature increase is 6°F. The maximum predicted temperature rise at the one Diesel Generator (DGE) air intake is 1°F (10,000 C/C_s = 3) Run 16, Table 6 (76). Usually it was much smaller.

5.4 Conclusions and Recommendations

It appears from the simulation and from the analysis of the results that 46-ft stacks will reduce the concentration ratio at the air intakes to acceptable levels at all wind speeds below U_R = 15 mph.

Higher concentrations, up to twice the permissible value, might occur at higher wind speeds from WD = 180° and WD = 202°.

According to Table 3b, the probability of such occurrences is limited to approximately 4.8 percent of the year. Since the wind speeds vary considerably within each day, it seems reasonable that one could schedule a testing program, according to the recorded distribution of wind speeds at the site, which will enable daily testing of the diesel generator without ever increasing the concentrations at the air intakes above the allowed values.

It should be stressed, however, that our estimates are based on an assumed correlation between the probabilities of wind speeds at the Meteorological Tower and the site of the LGS. It should also be kept in mind that the accuracy of such wind tunnel simulations is of the order of 20%. On the other hand, we have always referred to the maximum recorded concentrations at the neighborhood of each critical air intake and not to the average concentrations. Our conclusion is also based on the assumption that there are no strong inversions at the site which the plumes cannot penetrate.

The use of 27.5-ft stacks, rather than 46-ft stacks, appears to increase the probability of large concentrations considerably, as the critical wind speed for this case is U_R = 12 mph for WD = 180° and U_R = 14.5 for WD = 202° and 225°. It is quite possible that an analysis of the hourly wind-speed distributions at the site will indicate that an operation scheme for almost daily testing of the generators at lower speeds is attainable.

The above analysis is primarily based on the predicted high concentrations at either RBW or RBE. A considerable reduction in concentration in the Reactor Building Enclosure would occur if all the air intakes of the building will work together and the air inside the building will be adequately mixed. One should also examine the possibility of operating only the air intake at RBE at high wind speeds from WD = 180°, and operating RBW for high speed winds from WD = 225°.

REFERENCES

Cermak, J.E., "Applications of Fluid Mechanics to Wind Engineering - A Freeman Scholar Lecture," Transactions, ASME, J. of Fluid Engineering, Vol. 97, Mar., 1975, pp. 9-38.

Cermak, J. E., "Laboratory Simulation of Atmospheric Boundary Layer," AIAA J., Vol. 6, pp. 1746-1754 (1971).

Poreh, M. and A. Kacherginsky, "Simulation of Plume Rise Using Small Wind-Tunnel Models," J. of Wind Engineering and Industrial Aerodynamics, Vol. 7, pp. 1-14 (1981).

Guideline for Fluid Modeling to Determine Good Engineering Practice Stack Height (Draft) - EPA Publication, EPA-450-79-015, p. 27 (1979).

TABLES AND FIGURES

TABLE 1. SCALES IN THE LGS MODEL

Variable	Scale*
Geometry (L)	$R_L = 1/110$
Stack diameter (d) (0.375")	$R_d = 1/80$
Wind speeds (U_a)	$R(U_a) = 1/6.45$
Exit velocities for full load (V_{SF}) $V_{SFm} = 4.7$ m/sec	$R(V_{SF}) = 1/6.45$
Exit velocities for idling (V_{SI}) $V_{SIm} = 1.094$ m/sec	$R(V_{SI}) = 1/7.31$
Velocity ratios	$R(V_s)$
Discharge from stack (full load)	$R(Q_{SF}) = 1/41280$
Discharge from stack (idling)	$R(Q_{SI}) = 1/46784$
Discharge at air intakes and exhausts in building	$R_{QAC} = 1/78045$
Density ratio exit model plume (full load)	$(\rho_m/\rho_p)_{mF} = 0.242$
Density ratio exit model plume (idling)	$(\rho_m/\rho_p)_{mI} = 0.439$
Scale of density ratio (full-load)	$R(\rho_s/\rho_a)_F = 0.529$
Scale of density ratio (idling)	$R(\rho_s/\rho_a)_I = 0.680$
Scale of concentration dilutions (full scale)	$R(C/C_s)_F = 1.89$
Scale of concentration dilutions (idling)	$R(C/C_s)_I = 1.67$

*See definition of R on page 4.

TABLE 2. THE VELOCITY PROFILES FOR U_R = 127.7 CM/SEC

Data Point	Height cm	UMEAN cm/s	U-RMS cm/s	Turb Int percent
1	6.00	65.10	10.205	15.68
2	9.30	71.55	9.420	13.17
3	14.34	76.59	10.567	13.80
4	19.37	75.79	11.522	15.20
5	24.40	75.52	9.700	12.84
6	29.41	82.17	11.243	13.68
7	36.88	86.00	11.000	12.79
8	44.42	93.86	13.727	14.62
9	51.77	97.55	15.034	15.41
10	59.32	95.69	14.174	14.81
11	69.27	105.62	16.211	15.35
12	79.30	109.12	13.637	12.50
13	89.29	114.57	11.316	9.88
14	99.37	116.32	9.863	8.48
15	109.29	120.30	9.362	7.78
16	119.32	124.50	9.399	7.55
17	129.43	127.67	7.235	5.67
18	140.00	127.70	7.000	5.48

TABLE 3. PROBABILITY DISTRIBUTION OF WIND SPEEDS AT THE METEOROLOGICAL TOWER

a) 30 ft

SPEED RANGES (mph) DIRECTION vs. SPEED

DIRECTION	0-3 SUM	0-3 %	4-7 SUM	4-7 %	8-12 SUM	8-12 %	13-18 SUM	13-18 %	19-23 SUM	19-23 %	24+ SUM	24+ %	ALL SPEEDS SUM	ALL SPEEDS %
22.5	431	1.8	334	1.4	113	0.5	37	0.5	2	0.0	0	0.0	917	3.8
45.0	459	1.9	334	1.4	113	0.5	8	0.0	2	0.0	1	0.0	917	3.8
67.5	642	2.6	507	2.1	211	0.9	47	0.2	9	0.0	6	0.0	1422	5.9
90.0	838	3.5	713	2.9	306	1.3	63	0.3	2	0.0	0	0.0	1922	7.9
112.5	556	2.3	413	1.7	160	0.7	20	0.1	2	0.0	0	0.0	1150	4.7
135.0	547	2.3	370	1.5	94	0.4	19	0.1	0	0.0	0	0.0	1030	4.2
157.5	563	2.3	442	1.8	122	0.5	21	0.1	5	0.0	0	0.0	1153	4.8
180.0	699	2.9	646	2.7	280	1.2	28	0.1	4	0.0	0	0.0	1657	6.8
202.5	549	2.3	490	2.0	326	1.3	32 98	0.4	6.	0.0	0	0.0	1469	6.1
225.0	481	2.1	346	1.4	182	0.8	49	0.2	5	0.0	1	0.0	1064	4.4
247.5	520	2.1	420	1.7	231	1.0	57	0.2	5	0.0	1	0.1	1234	5.1
270.0	663	2.7	594	2.5	417	1.7	217	0.9	71	0.3	28	0.1	1990	8.2
292.5	813	3.4	968	4.0	851	3.5	564	2.3	171	0.7	31	0.0	3398	14.0
315.0	673	2.8	647	2.7	545	2.2	468	1.9	101	0.4	6	0.0	2440	10.1
337.5	495	2.0	337	1.4	335	1.4	152	0.6	18	0.1	1	0.0	1336	5.5
360.0	471	1.9	415	1.7	206	0.8	42	0.2	1	0.0	0	0.0	1135	4.7
	9400/38.8		7976/32.9		4492/18.7		1890/ 7.8		403/ 1.5		75/ .2		24234/ 87.4	

Mean wind speed: 5.8

Total number of uninteruptable hours: 55

Total number of calm hours: 2570, Percent: 10.6

Missing speeds: 1364 Percent: 5.6

Missing directions: 1586 Percent: 6.5

(1) Period of data: 1/72 - 12/74, data taken at 30 ft level

b) 270 ft

Wind Speed (mi/hr)

Direction	0-3	4-7	8-12	13-18	19-23	24+	Total
22.5	0.506%	0.906%	1.337%	0.577%	0.062%	0.012%	3.400%
45.0	0.457%	1.013%	1.342%	0.516%	0.073%	0.031%	3.431%
67.5	0.563%	1.304%	1.543%	0.644%	0.106%	0.064%	4.223%
90.0	0.641%	1.687%	2.120%	0.994%	0.097%	0.021%	5.560%
112.5	0.424%	1.093%	1.313%	0.712%	0.073%	0.009%	3.625%
135.0	0.466%	1.105%	1.389%	0.513%	0.066%	0.021%	3.516%
157.5	0.523%	1.240%	1.746%	0.618%	0.092%	0.057%	4.275%
180.0	0.819%	2.058%	2.806%	1.223%	0.244%	0.078%	7.228%
202.5	0.800%	1.857%	2.404%	1.405%	0.367%	0.156%	6.989%
225.0	0.684%	2.070%	1.987%	0.743%	0.151%	0.054%	5.690%
247.5	0.686%	1.791%	1.855%	0.731%	0.187%	0.125%	5.375%
270.0	0.816%	2.619%	2.983%	1.980%	0.547%	0.556%	9.502%
292.5	0.774%	2.792%	4.888%	4.457%	1.720%	1.446%	16.077%
315.0	0.684%	1.746%	2.950%	3.573%	1.370%	0.892%	11.215%
337.5	0.490%	1.072%	1.595%	1.422%	0.471%	0.135%	5.184%
360.0	0.516%	1.263%	1.580%	1.126%	0.156%	0.024%	4.666%
	9.847%	25.616%	33.838%	21.235%	5.782%	3.681%	100.000%

TABLE 4. THE FLOW VISUALIZATION PROGRAM

Run	Wind Direction (WD)	Stacks H (ft)	Reference Prototype Wind Speed U_R (mph)	Load	Unit No.
1	180	7.5 N*	8	Idle	1
2	180	7.5 N	12	Idle	1
3	180	7.5	8	Idle	1
4	180	7.5	12	Idle	1
5	180	17.5	8	Idle	1
6	180	17.5	12	Idle	1
7	180	27.5	8	Idle	1
8	180	27.5	12	Idle	1
9	180	46	8	Idle	1
10	180	46	12	Idle	1
11	180	7.5 N	8	Full	1
12	180	7.5 N	12	Full	1
13	180	7.5	8 and 12	Full	1
14	180	17.5	8 and 12	Full	1
15	180	27.5	8 and 12	Full	1
16	180	46	8 and 12	Full	1
17	202	46	16	Full	1
18	360	46	16	Full	1
19	67	46	12	Idle	1
20	292	46	16	Idle	1
21	300	2	16	Full	1
22	315	2	16	Full	1
23	202	2	16	100%	1
24	180	2	12	100%	1
25	180	2	12	100%	2
26	157	2	12	100%	2
27	60	2	12	100%	2
28	45	2	12	100%	2

*Exit oriented to North.

TABLE 5. SUMMARY OF THE CONCENTRATION MEASUREMENTS

a. H = 46 ft, Full Load, Unit 1

No. at Table 6	Run No.	Operating Stacks	Wind Direction	Reference Wind Speed (mph)	Critical C/C_s at:
1	101	1-4	180	9	--
2	108	1-4	180	14	--
3	103	1-4	180	16	RBW
4	107	1-4	180	16	RBW
5	102	1-4	180	18.3	RBW
6	104	1-4	180	21	RBW
7	113	1-4	180	21.5	RBW
8	114	1-4	180	21.5	RBW
9	105	1-4	180	26	RBW
10	106	1-4	180	30	RBW
--	--	--	--	--	--
11	110	1	180	21.5	RBW
12	116	1	180	21.5	--
13	112	2	180	21.5	RBW
14	118	2	180	21.5	RBW
15	208	3	180	16	RBW
16	111	3	180	21.5	RBW
17	117	3	180	21.5	RBW
18	115	4	180	21.5	RBW
19	109	4	180	21.5	RBW
--	--	--	--	--	--
20	127	1-4	202	16	--
21	126	1-4	202	22.5	RBW,RBE
22	169	1-4	247	21	--
23	166	1-4	270	21.3	--
24	164	1-4	292	21.3	--
25	199	1-4	300	10.8	--
26	158	1-4	300	16	--
27	157	1-4	300	21	--
28	162	1	300	27.5	--
29	130	1-4	315	21	--
30	131	1	315	21.5	--
31	129	1-4	337	21	--
32	128	1-4	360	21.5	--

TABLE 5 (CONTINUED)

b. H = 27.5, Full Load

No. at Table 6	Run No.	Operating Stacks	Wind Direction	Reference Wind Speed (mph)	Critical C/C_s at:
33	211	3	180	11.7	--
34	212	3	180	12.6	--
35	210	3	180	14	RBW
36	209	3	180	16	RBW
37	202	1-4	180	12.6	--
38	201	1-4	180	15	RBW
39	200	1-4	180	18	RBW
40	119	1-4	180	21.5	RBW
--	--	--	--	--	--
41	199	1-4	202	14	--
42	202	1-4	202	16	RBE
43	197	1-4	202	18.5	RBW,RBE
44	178	1-4	225	14	--
45	177	1-4	225	16	RBE
46	176	1-4	225	18	RBE
47	175	1-4	225	21	RBE
48	180	1	225	16	--
49	179	1	225	18	RBE
50	173	1-4	247	12.5	--
51	174	1-4	247	14	--
52	172	1-4	247	16.5	--
53	171	1-4	247	18	--
54	170	1-4	247	21	--
55	160	1-4	300	22.5	--
56	161	1	300	21.3	--

TABLE 5 (CONTINUED)

c. H = 46 ft.; Idle

No. at Table 6	Run No.	Operating Stacks	Wind Direction	Reference Wind Speed (mph)	Critical C/C_s at:
57	125	1-4	180	7	--
58	124	1-4	180	10	--
59	123	1-4	180	13.8	--
60	122	1-4	180	17	RBW
61	121	1-4	180	21	RBW
62	170	1-4	180	25.6	--

d. H = 2.5 ft.; Full Load

No. at Table 6	Run No.	Operating Stacks	Wind Direction	Reference Wind Speed (mph)	Critical C/C_s at:
63	206	1-4	180	9	--
64	207	1-4	180	10.3	--
65	205	1-4	180	12.2	RBW
66	204	1-4	180	12.2	RBW
67	203	1-4	180	14.6	RBW
68	195	1-4	202	11.7	RBW
69	196	1-4	202	18	RBW,RBE,AD
70	194	1-4	225	11.7	--
71	193	1-4	225	15	RBE
72	192	1-4	225	18	RBE
73	181	1-4	225	21	RBE,AD
74	168	1-4	247	21	--
75	167	1-4	270	21.3	--
76	165	1-4	292	21.3	RBE,AD
77	163	1-4	300	22.5	--
78	156	1-4	315	11	--
79	155	1-4	315	16	--
80	154	1-4	315	21	--
81	153	1-4	337	21.5	--
82	152	1-4	360	16	RBW
83	151	1-4	360	21.5	RBW

TABLE 6. MEASURED MODEL CONCENTRATIONS AND CALCULATED PROTOTYPE DILUTIONS

1

Run: 101
Wind Direction (°): 180
Ref. Wind Speed (mph): 9
Operating Stacks: 1, 2, 3, 4
Unit: 1
Stacks Height (ft): 46
Load: 100%

Location (see figure 8)		C ppm	C/C_s (P) x 10,000
RBW	1	2	0
	2	2	0
	3	1	0
	4	1	0
	5	1	0
	6	1	0
RBE	1	1	0
	2	1	0
	3	1	0
	4	1	0
RD		1	0
TBW		1	0
TBE		1	0
AD		1	0
CR		1	0
DGW		1	0
DGE	1	1	0
	2	--	--

2

Run: 108
Wind Direction (°): 180
Ref. Wind Speed (mph): 14
Operating Stacks: 1,2, 3, 4
Unit: 1
Stacks Height (ft): 46
Load: 100%

Location (see figure 8)		C ppm	C/C_s (P) x 10,000
RBW	1	158	42
	2	134	35
	3	147	39
	4	126	33
	5	143	38
	6	114	30
RBE	1	28	7
	2		
	3		
	4	20	5
RD			
TBW			
TBE			
AD			
CR			
DGW			
DGE	1		
	2		

3

Run: 103
Wind Direction (°): 180
Ref. Wind Speed (mph): 16
Operating Stacks: 1, 2, 3, 4
Unit: 1
Stacks Height (ft): 46
Load: 100%

Location (see figure 8)		C ppm	C/C_s (P) x 10,000
RBW	1	435	115
	2	382	101
	3	359	95
	4	357	94
	5	389	103
	6	361	96
RBE	1	64	17
	2	38	10
	3	32	8
	4	51	13
RD		7	2
TBW		8	2
TBE		6	1
AD		5	1
CR		24	6
DGW		9	2
DGE	1	--	--
	2	--	--

TABLE 6. MEASURED MODEL CONCENTRATIONS AND CALCULATED PROTOTYPE DILUTIONS

	4		5		6	
	Run: 107 Wind Direction (°): 180 Ref. Wind Speed (mph): 16 Operating Stacks: 1, 2, 3, 4 Unit: 1 Stacks Height (ft): 46 Load: 100%		Run: 102 Wind Direction (°): 180 Ref. Wind Speed (mph): 18.3 Operating Stacks: 1, 2, 3, 4 Unit: 1 Stacks Height (ft): 46 Load: 100%		Run: 104 Wind Direction (°): 180 Ref. Wind Speed (mph): 21 Operating Stacks: 1, 2, 3, 4 Unit: 1 Stacks Height (ft): 46 Load: 100%	
Location (see figure 8)	C ppm	C/C_s (P) x 10,000	C ppm	C/C_s (P) x 10,000	C ppm	C/C_s (P) x 10,000
RBW 1	394	104	433	115	685	181
2	354	94	405	107	718	190
3	385	102	406	107	597	158
4	345	91	400	106	693	183
5	360	95	375	99	662	175
6	265	70	374	99	721	191
RBE 1	62	16	60	16	111	29
2			27	7	59	16
3			20	5	46	12
4			47	12	95	25
			11	3		
RD			18	5	33	9
TBW			18	5	79	21
TBE			5	1	13	3
AD			5	1	11	3
CR			34	9	39	10
DGW			13	3	21	6
DGE 1			11	3	26	7
2			--	--	--	--

TABLE 6 (CONTINUED)

7

Run: 113
Wind Direction (°): 180
Ref. Wind Speed (mph): 21.5
Operating Stacks: 1, 2, 3, 4
Unit: 1
Stacks Height (ft): 46
Load: 100%

Location (see figure 8)		C ppm	C/C_s (P) x 10,000
RBW	1	761	201
	2	754	199
	3	712	188
	4	709	188
	5	753	199
	6	700	185
RBE	1	134	35
	2	70	19
	3	58	15
	4	95	25
RD			
TBW			
TBE			
AD			
CR			
DGW			
DGE	1		
	2		

8

Run: 114
Wind Direction (°): 180°
Ref. Wind Speed (mph): 21.5
Operating Stacks: 1, 2, 3, 4
Unit: 1
Stacks Height (ft): 46
Load: 100%

Location (see figure 8)		C ppm	C/C_s (P) x 10,000
RBW	1	781	207
	2	666	176
	3	682	180
	4	720	190
	5	735	194
	6	711	188
RBE	1	88	23
	2	60	16
	3	29	8
	4	69	18
RD			
TBW			
TBE			
AD			
CR			
DGW			
DGE	1		
	2		

9

Run: 105
Wind Direction (°): 180°
Ref. Wind Speed (mph): 26
Operating Stacks: 1, 2, 3, 4
Unit: 1
Stacks Height (ft): 46
Load: 100%

Location (see figure 8)		C ppm	C/C_s (P) x 10,000
RBW	1	694	184
	2	561	148
	3	523	138
	4	679	180
	5	709	188
	6	703	186
RBE	1	54	14
	2	34	9
	3	26	7
	4	50	13
RD		80	21
TBW		137	36
TBE		12	3
AD		15	4
CR		49	13
DGW		24	6
DGE	1	33	9
	2	--	--

TABLE 6 (CONTINUED)

10				11				12			
Run: 106 Wind Direction (°): 180 Ref. Wind Speed (mph): 30 Operating Stacks: 1, 2, 3, 4 Unit: 1 Stacks Height (ft): 46 Load: 100%				Run: 110 Wind Direction (°): 180° Ref. Wind Speed (mph): 21.5 Operating Stacks: 1 Unit: 1 Stacks Height (ft): 46 Load: 100%				Run: 116 Wind Direction (°): 180° Ref. Wind Speed (mph): 21.5 Operating Stacks: 1, 2, 3 Unit: 1 Stacks Height (ft): 46 Load: 100%			
Location (see figure 8)		C ppm	C/C_s (P) x 10,000	Location (see figure 8)		C ppm	C/C_s (P) x 10,000	Location (see figure 8)		C ppm	C/C_s (P) x 10,000
RBW	1	726	192	RBW	1	87	23	RBW	1	85	22
	2	631	167		2	21	6		2	39	10
	3	632	167		3	11	3		3	30	8
	4	611	162		4	24	6		4	44	12
	5	679	180		5	47	12		5	62	16
	6	635	168		6	136	36		6	67	17
RBE	1	93	25	RBE	1	1	0	RBE	1	1	0
	2				2	0	0		2	1	0
	3				3	0	0		3	1	0
	4				4	0	0		4	1	0
RD				RD				RD			
TBW				TBW				TBW			
TBE				TBE				TBE			
AD				AD				AD			
CR				CR				CR			
DGW				DGW				DGW			
DGE	1			DGE	1			DGE	1		
	2				2				2		

TABLE 6 (CONTINUED)

13

Run: 112
Wind Direction (°): 180
Ref. Wind Speed (mph): 21.5
Operating Stacks: 2
Unit: 1
Stacks Height (ft): 46
Load: 100%

Location (see figure 8)		C ppm	C/C_s (P) x 10,000
RBW	1	163	40
	2	54	14
	3	34	9
	4	85	22
	5	150	40
	6	173	46
RBE	1	0	0
	2	0	0
	3	0	0
	4	0	0
RD			
TBW			
TBE			
AD			
CR			
DGW			
DGE	1		
	2		

14

Run: 118
Wind Direction (°): 180
Ref. Wind Speed (mph): 21.5
Operating Stacks: 2
Unit: 1
Stacks Height (ft): 46
Load: 100%

Location (see figure 8)		C ppm	C/C_s (P) x 10,000
RBW	1	94	25
	2	51	13
	3	34	9
	4	68	19
	5	94	25
	6	104	28
RBE	1	1	0
	2	1	0
	3	0	0
	4	1	0
RD			
TBW			
TBE			
AD			
CR			
DGW			
DGE	1		
	2		

15

Run: 208
Wind Direction (°): 180
Ref. Wind Speed (mph): 16
Operating Stacks: 3
Unit: 1
Stacks Height (ft): 46
Load: 100%

Location (see figure 8)		C ppm	C/C_s (P) x 10,000
RBW	1	67	18
	2	93	25
	3	96	25
	4	116	31
	5	65	17
	6	65	17
RBE	1		
	2		
	3		
	4		
RD			
TBW			
TBE			
AD			
CR			
DGW			
DGE	1		
	2		

TABLE 6 (CONTINUED)

16

Run: 111
Wind Direction (°): 180
Ref. Wind Speed (mph): 21.5
Operating Stacks: 3
Unit: 1
Stacks Height (ft): 46
Load: 100%

Location (see figure 8)		C ppm	C/C_s (P) x 10,000
RBW	1	129	34
	2	157	42
	3	121	32
	4	157	42
	5	143	38
	6	136	36
RBE	1	16	4
	2	8	2
	3	5	1
	4	14	4
RD			
TBW			
TBE			
AD			
CR			
DGW			
DGE	1		
	2		

17

Run: 117
Wind Direction (°): 180
Ref. Wind Speed (mph): 21.5
Operating Stacks: 3
Unit: 1
Stacks Height (ft): 46
Load: 100%

Location (see figure 8)		C ppm	C/C_s (P) x 10,000
RBW	1	105	28
	2	165	44
	3	150	40
	4	154	41
	5	93	25
	6	81	21
RBE	1	31	8
	2		
	3		
	4		
RD			
TBW			
TBE			
AD			
CR			
DGW			
DGE	1		
	2		

18

Run: 115
Wind Direction (°): 180
Ref. Wind Speed (mph): 21.5
Operating Stacks: 4
Unit: 1
Stacks Height (ft): 46
Load: 100%

Location (see figure 8)		C ppm	C/C_s (P) x 10,000
RBW	1	114	30
	2	173	46
	3	187	49
	4	138	37
	5	104	28
	6	97	26
RBE	1	51	13
	2	21	6
	3	14	4
	4	34	9
RD			
TBW			
TBE			
AD			
CR			
DGW			
DGE	1		
	2		

TABLE 6 (CONTINUED)

19

Run: 109
Wind Direction (°): 180
Ref. Wind Speed (mph): 21.5
Operating Stacks: 4
Unit: 1
Stacks Height (ft): 46
Load: 100%

Location (see figure 8)		C ppm	C/C_s (P) x 10,000
RBW	1	98	26
	2	140	37
	3	153	40
	4	109	29
	5	128	34
	6	84	22
RBE	1	59	16
	2	35	9
	3	15	4
	4	40	11
RD			
TBW			
TBE			
AD			
CR			
DGW			
DGE	1		
	2		

20

Run: 127
Wind Direction (°): 202
Ref. Wind Speed (mph): 16
Operating Stacks: 1, 2, 3, 4
Unit: 1
Stacks Height (ft): 46
Load: 100%

Location (see figure 8)		C ppm	C/C_s (P) x 10,000
RBW	1	3	1
	2	16	4
	3	34	9
	4	15	4
	5	6	2
	6	4	1
RBE	1	121	32
	2	73	19
	3	66	17
	4	91	24
RD		0	0
TBW		0	0
TBE		17	4
AD		14	4
CR		41	11
DGW		3	1
DGE	1	1	0
	2		

21

Run: 126
Wind Direction (°): 202
Ref. Wind Speed (mph): 22.5
Operating Stacks: 1, 2, 3, 4
Unit: 1
Stacks Height (ft): 46
Load: 100%

Location (see figure 8)		C ppm	C/C_s (P) x 10,000
RBW	1	249	66
	2	404	107
	3	533	141
	4	397	105
	5	275	73
	6	217	57
RBE	1	428	113
	2	258	68
	3	250	66
	4	341	90
RD		9	2
TBE		6	2
TBE		72	19
AD		60	16
CR		75	20
DGW		19	5
DGE	1	24	6
	2		

TABLE 6 (CONTINUED)

22

Run: 169
Wind Direction (°): 247.5
Ref. Wind Speed (mph): 21
Operating Stacks: 1, 2, 3, 4
Unit: 1
Stacks Height (ft): 46
Load: 100%

Location (see figure 8)		C ppm	C/C_s (P) x 10,000
RBW	1	0	0
	2	0	0
	3		
	4		
	5		
	6		
RBE	1	31	8
	2	70	19
	3		
	4		
RD		0	0
TBW		0	0
TBE		10	3
AD		11	3
CR		0	0
DGW		1	0
DGE	1	0	0
	2	0	0

23

Run: 166
Wind Direction (°): 270
Ref. Wind Speed (mph): 21.3
Operating Stacks: 1, 2, 3, 4
Unit: 1
Stacks Height (ft): 46
Load: 100%

Location (see figure 8)		C ppm	C/C_s (P) x 10,000
RBW	1	1	0
	2	1	0
	3		
	4		
	5		
	6		
RBE	1	9	2
	2	23	6
	3		
	4		
RD		0	0
TBW		0	0
TBE		10	3
AD		10	3
CR		0	0
DGW		1	0
DGE	1	1	0
	2	1	0

24

Run: 164
Wind Direction (°): 292
Ref. Wind Speed (mph): 21.3
Operating Stacks: 1, 2, 3, 4
Unit: 1
Stacks Height (ft): 46
Load: 100%

Location (see figure 8)		C ppm	C/C_s (P) x 10,000
RBW	1	46	12
	2	92	24
	3		
	4		
	5		
	6		
RBE	1	144	38
	2	130	34
	3		
	4		
RD		0	0
TBW		0	0
TBE		94	25
AD		73	19
CR		0	0
DGW		3	1
DGE	1	15	4
	3	14	4

TABLE 6 (CONTINUED)

25

Run: 159
Wind Direction (°): 300
Ref. Wind Speed (mph): 10.8
Operating Stacks: 1, 2, 3, 4
Unit: 1
Stacks Height (ft): 46
Load: 100%

Location (see figure 8)		C ppm	C/C_s (P) x 10,000
RBW	1	7	2
	2	42	11
	3		
	4		
	5		
	6		
RBE	1	16	4
	2	15	4
	3		
	4		
RD		0	0
TBW		0	0
TBE		8	2
AD		7	2
CR		0	0
DGW		1	0
DGE	1	3	1
	2	7	2

26

Run: 158
Wind Direction (°): 300
Ref. Wind Speed (mph): 16
Operating Stacks: 1, 2, 3, 4
Unit: 1
Stacks Height (ft): 46
Load: 100%

Location (see figure 8)		C ppm	C/C_s (P) x 10,000
RBW	1	43	11
	2	92	24
	3		
	4		
	5		
	6		
RBE	1	64	17
	2	55	15
	3		
	4		
RD		0	0
TBW		0	0
TBE		26	7
AD		23	6
CR		0	0
DGW		7	2
DGE	1	16	4
	2	35	9

27

Run: 157
Wind Direction (°): 300
Ref. Wind Speed (mph): 21
Operating Stacks: 1, 2, 3, 4
Unit: 1
Stacks Height (ft): 46
Load: 100%

Location (see figure 8)		C ppm	C/C_s (P) x 10,000
RBW	1	98	26
	2	169	45
	3		
	4		
	5		
	6		
RBE	1	117	31
	2	110	29
	3		
	4		
RD		0	0
TBW		0	0
TBE		48	13
AD		42	11
CR		1	0
DGW		10	3
DGE	1	29	8
	2	64	17

TABLE 6 (CONTINUED)

28

Run: 162
Wind Direction (°): 300
Ref. Wind Speed (mph): 22.5
Operating Stacks: 1
Unit: 1
Stacks Height (ft): 46
Load: 100%

Location (see figure 8)		C ppm	C/C_s (P) x 10,000
RBW	1	35	9
	2	60	16
	3		
	4		
	5		
	6		
RBE	1	61	16
	2	59	16
	3		
	4		
RD		0	0
TBW		0	0
TBE		27	7
AD		24	6
CR		0	0
DGW		4	1
DGE	1	13	3
	2	29	8

29

Run: 130
Wind Direction (°): 315
Ref. Wind Speed (mph): 21
Operating Stacks: 1, 2, 3, 4
Unit: 1
Stacks Height (ft): 46
Load: 100%

Location (see figure 8)		C ppm	C/C_s (P) x 10,000
RBW	1	64	17
	2	58	15
	3		
	4		
	5		
	6		
RBE	1	58	15
	2	54	14
	3		
	4		
RD		0	0
TBW		0	0
TBE		31	8
AD		29	8
CR		0	0
DGW		10	3
DGE	1	26	7
	2	51	13

30

Run: 131
Wind Direction (°): 315
Ref. Wind Speed (mph): 21.5
Operating Stacks: 1
Unit: 1
Stacks Height (ft): 46
Load: 100%

Location (see figure 8)		C ppm	C/C_s (P) x 10,000
RBW	1	43	11
	2	38	10
	3		
	4		
	5		
	6		
RBE	1	35	9
	2	33	9
	3		
	4		
RD		0	0
TBW		0	0
TBE		18	5
AD		17	5
CR		0	0
DGW		7	2
DGE	1	14	4
	2	30	8

TABLE 6 (CONTINUED)

31

Run: 129
Wind Direction (°): 337
Ref. Wind Speed (mph): 21
Operating Stacks: 1, 2, 3, 4
Unit: 1
Stacks Height (ft): 46
Load: 100%

Location (see figure 8)		C ppm	C/C_s (P) x 10,000
RBW	1	37	10
	2	36	10
	3		
	4		
	5		
	6		
RBE	1	36	10
	2	33	9
	3		
	4		
RD		0	0
TBW		0	0
TBE		22	6
AD		21	6
CR		0	0
DGW		7	2
DGE	1	17	4
	2	32	8

32

Run: 128
Wind Direction (°): 360
Ref. Wind Speed (mph): 21.5
Operating Stacks: 1, 2, 3, 4
Unit: 1
Stacks Height (ft): 46
Load: 100%

Location (see figure 8)		C ppm	C/C_s (P) x 10,000
RBW	1	36	10
	2	30	8
	3		
	4		
	5		
	6		
RBE	1	21	6
	2	20	5
	3		
	4		
RD		1	0
TBW		21	6
TBE		6	2
AD		5	1
CR		0	0
DGW		17	4
DGE	1	5	1
	2	5	1

Run:
Wind Direction (°):
Ref. Wind Speed (mph):
Operating Stacks:
Unit:
Stacks Height (ft):
Load:

Location (see figure 8)		C ppm	C/C_s (P) x 10,000
RBW	1		
	2		
	3		
	4		
	5		
	6		
RBE	1		
	2		
	3		
	4		
RD			
TBW			
TBE			
AD			
CR			
DGW			
DGE	1		
	2		

TABLE 6 (CONTINUED)

33

Run: 211
Wind Direction (°): 180
Ref. Wind Speed (mph): 11.7
Operating Stacks: 3
Unit: 1
Stacks Height (ft): 27.5
Load: 100%

Location (see figure 8)		C ppm	C/C_s (P) x 10,000
RBW	1	12	3
	2	0	0
	3	0	0
	4	4	1
	5	22	6
	6	13	3
RBE	1		
	2		
	3		
	4		
RD			
TBW			
TBE			
AD			
CR			
DGW			
DGE	1		
	2		

34

Run: 212
Wind Direction (°): 180
Ref. Wind Speed (mph): 12.6
Operating Stacks: 3
Unit: 1
Stacks Height (ft): 27.5
Load: 100%

Location (see figure 8)		C ppm	C/C_s (P) x 10,000
RBW	1	84	22
	2	50	13
	3	62	16
	4	81	21
	5	88	23
	6	86	23
RBE	1		
	2		
	3		
	4		
RD			
TBW			
TBE			
AD			
CR			
DGW			
DGE	1		
	2		

35

Run: 210
Wind Direction (°): 180
Ref. Wind Speed (mph): 14
Operating Stacks: 3
Unit: 1
Stacks Height (ft): 27.5
Load: 100%

Location (see figure 8)		C ppm	C/C_s (P) x 10,000
RBW	1	194	51
	2	175	46
	3	145	38
	4	218	58
	5	217	57
	6	182	48
RBE	1		
	2		
	3		
	4		
RD			
TBW			
TBE			
AD			
CR			
DGW			
DGE	1		
	2		

TABLE 6 (CONTINUED)

36

Run: 209
Wind Direction (°): 180
Ref. Wind Speed (mph): 16
Operating Stacks: 3
Unit: 1
Stacks Height (ft): 27.5
Load: 100%

Location (see figure 8)		C ppm	C/C_s (P) x 10,000
RBW	1	216	57
	2	283	75
	3	319	84
	4	275	73
	5	193	51
	6	153	40
RBE	1		
	2		64
	3		
	4		
RD			
TBW			
TBE			
AD			
CR			
DGW			
DGE	1		
	2		

37

Run: 202
Wind Direction (°): 180
Ref. Wind Speed (mph): 12.6
Operating Stacks: 1, 2, 3, 4
Unit: 1
Stacks Height (ft): 27.5
Load: 100%

Location (see figure 8)		C ppm	C/C_s (P) x 10,000
RBW	1	209	55
	2	175	46
	3		
	4		
	5		
	6		
RBE	1		
	2		
	3		
	4		
RD			
TBW			
TBE			
AD			
CR			
DGW			
DGE	1		
	2		

38

Run: 201
Wind Direction (°): 180
Ref. Wind Speed (mph): 15
Operating Stacks: 1, 2, 3, 4
Unit: 1
Stacks Height (ft): 27.5
Load: 100%

Location (see figure 8)		C ppm	C/C_s (P) x 10,000
RBW	1	686	181
	2	566	150
	3		
	4		
	5		
	6		
RBE	1	77	20
	2	44	12
	3		
	4		
RD			
TBW			
TBE			
AD			
CR			
DGW			
DGE	1		
	2		

TABLE 6 (CONTINUED)

39

Run: 200
Wind Direction (°): 180
Ref. Wind Speed (mph): 18
Operating Stacks: 1, 2, 3, 4
Unit: 1
Stacks Height (ft): 27.5
Load: 100%

Location (see figure 8)		C ppm	C/C_s (P) x 10,000
RBW	1	979	259
	2	879	233
	3		
	4		
	5		
	6		
RBE	1	168	44
	2	98	26
	3	119	31
	4		
RD		15	4
TBW		63	17
TBE		14	4
AD		12	3
CR		40	11
DGW		18	5
DGE	1	22	6
	2	15	4

40

Run: 119
Wind Direction (°): 180
Ref. Wind Speed (mph): 21.5
Operating Stacks: 1, 2, 3, 4
Unit: 1
Stacks Height (ft): 27.5
Load: 100%

Location (see figure 8)		C ppm	C/C_s (P) x 10,000
RBW	1	1053	279
	2	984	260
	3	995	263
	4	1012	268
	5	998	264
	6	965	255
RBE	1	175	46
	2	88	23
	3	70	19
	4	152	40
RD			
TBW			
TBE			
AD			
CR			
DGW			
DGE	1		
	2		

41

Run: 199
Wind Direction (°): 202
Ref. Wind Speed (mph): 14
Operating Stacks: 1, 2, 3, 4
Unit: 1
Stacks Height (ft): 27.5
Load: 100%

Location (see figure 8)		C ppm	C/C_s (P) x 10,000
RBW	1	69	18
	2	195	52
	3		
	4		
	5		
	6		
RBE	1	168	39
	2	111	29
	3	122	32
	4		
RD		0	0
TBW		1	0
TBE		18	5
AD		12	3
CR		48	13
DGW		7	2
DGE	1	4	1
	2	4	1

TABLE 6 (CONTINUED)

42

Run: 198
Wind Direction (°): 202
Ref. Wind Speed (mph): 16
Operating Stacks: 1, 2, 3, 4
Unit: 1, 2
Stacks Height (ft): 27.5
Load: 100%

Location (see figure 8)		C ppm	C/C_s (P) x 10,000
RBW	1	79	21
	2	263	70
	3		
	4		
	5		
	6		
RBE	1	498	132
	2	297	79
	3	430	114
	4		
RD		0	0
TBW		0	0
TBE		55	15
AD		49	13
CR		46	12
DGW		13	3
DGE	1	5	1
	2	5	1

43

Run: 197
Wind Direction (°): 202
Ref. Wind Speed (mph): 18.5
Operating Stacks: 1, 2, 3, 4
Unit: 1
Stacks Height (ft): 27.5
Load: 100%

Location (see figure 8)		C ppm	C/C_s (P) x 10,000
RBW	1	219	58
	2	538	142
	3		
	4		
	5		
	6		
RBE	1	672	178
	2	464	123
	3	556	147
	4		
RD		3	1
TBW		3	1
TBE		82	22
AD		76	20
CR		56	15
DGW		25	7
DGE	1	22	6
	2	12	3

44

Run: 178
Wind Direction (°): 225
Ref. Wind Speed (mph): 14
Operating Stacks: 1, 2, 3, 4
Unit: 1
Stacks Height (ft): 27.5
Load: 100%

Location (see figure 8)		C ppm	C/C_s (P) x 10,000
RBW	1	1	0
	2	1	0
	3		
	4		
	5		
	6		
RBE	1	49	13
	2	51	13
	3		
	4		
RD		0	0
TBW		5	1
TBE		5	1
AD		4	1
CR		0	0
DGW		2	1
DGE	1	1	0
	2	1	0

TABLE 6 (CONTINUED)

45

Run: 177
Wind Direction (°): 225
Ref. Wind Speed (mph): 16
Operating Stacks: 1, 2, 3, 4
Unit: 1
Stacks Height (ft): 27.5
Load: 100%

Location (see figure 8)		C ppm	C/C_s (P) x 10,000
RBW	1	0	0
	2	5	1
	3		
	4		
	5		
	6		
RBE	1	524	139
	2	435	115
	3		
	4		
RD		0	0
TBW		0	0
TBE		35	9
AD		44	12
CR		4	1
DGW		11	3
DGE	1	4	1
	2	6	2

46

Run: 176
Wind Direction (°): 225
Ref. Wind Speed (mph): 18
Operating Stacks: 1, 2, 3, 4
Unit: 1
Stacks Height (ft): 27.5
Load: 100%

Location (see figure 8)		C ppm	C/C_s (P) x 10,000
RBW	1	1	0
	2	36	10
	3		
	4		
	5		
	6		
RBE	1	654	173
	2	560	148
	3		
	4		
RD		0	0
TBW		0	0
TBE		67	18
AD		82	22
CR		3	1
DGW		13	3
DGE	1	5	1
	2	6	2

47

Run: 175
Wind Direction (°): 225
Ref. Wind Speed (mph): 21
Operating Stacks: 1, 2, 3, 4
Unit: 1
Stacks Height (ft): 27.5
Load: 100%

Location (see figure 8)		C ppm	C/C_s (P) x 10,000
RBW	1	4	1
	2	19	5
	3		
	4		
	5		
	6		
RBE	1	584	154
	2	469	124
	3		
	4		
RD		0	0
TBW		0	0
TBE		63	17
AD		76	20
CR		2	1
DGW		13	3
DGE	1	4	1
	2	6	1

TABLE 6 (CONTINUED)

48

Run: 180
Wind Direction (°): 225
Ref. Wind Speed (mph): 16
Operating Stacks: 1
Unit: 1
Stacks Height (ft): 27.5
Load: 100%

Location (see figure 8)		C ppm	C/C_s (P) x 10,000
RBW	1	0	0
	2	0	0
	3		
	4		
	5		
	6		
RBE	1	86	23
	2	83	22
	3		
	4		
RD		0	0
TBW		0	0
TBE		8	2
AD		11	3
CR		1	0
DGW		3	1
DGE	1	1	0
	2	2	1

49

Run: 179
Wind Direction (°): 225
Ref. Wind Speed (mph): 18
Operating Stacks: 1
Unit: 1
Stacks Height (ft): 27.5
Load: 100%

Location (see figure 8)		C ppm	C/C_s (P) x 10,000
RBW	1	0	0
	2	0	0
	3		
	4		
	5		
	6		
RBE	1	108	29
	2	112	30
	3		
	4		
RD		0	0
TBW		0	0
TBE		13	3
AD		17	4
CR		1	0
DGW		3	1
DGE	1	1	0
	2	2	1

50

Run: 173
Wind Direction (°): 247
Ref. Wind Speed (mph): 12.5
Operating Stacks: 1, 2, 3, 4
Unit: 1
Stacks Height (ft): 27.5
Load: 100%

Location (see figure 8)		C ppm	C/C_s (P) x 10,000
RBW	1	0	0
	2	0	0
	3		
	4		
	5		
	6		
RBE	1	1	0
	2	3	1
	3		
	4		
RD		0	0
TBW		0	0
TBE		1	0
AD		1	0
CR		0	0
DGW		0	0
DGE	1	0	0
	2	0	0

TABLE 6 (CONTINUED)

51

Run: 174
Wind Direction (°): 247
Ref. Wind Speed (mph): 14
Operating Stacks: 1, 2, 3, 4
Unit: 1
Stacks Height (ft): 27.5
Load: 100%

Location (see figure 8)		C ppm	C/C_s (P) x 10,000
RBW	1	0	0
	2	0	0
	3		
	4		
	5		
	6		
RBE	1	21	6
	2	24	6
	3		
	4		
RD		0	0
TBW		0	0
TBE		3	1
AD		2	1
CR		0	0
DGW		1	0
DGE	1	0	0
	2	0	0

52

Run: 172
Wind Direction (°): 247
Ref. Wind Speed (mph): 16.5
Operating Stacks: 1, 2, 3, 4
Unit: 1
Stacks Height (ft): 27.5
Load: 100%

Location (see figure 8)		C ppm	C/C_s (P) x 10,000
RBW	1	0	0
	2	0	0
	3		
	4		
	5		
	6		
RBE	1	101	27
	2	148	39
	3		
	4		
RD		0	0
TBW		0	0
TBE		12	3
AD		13	3
CR		0	0
DGW		3	1
DGE	1	0	0
	2	1	0

53

Run: 171
Wind Direction (°): 247
Ref. Wind Speed (mph): 18
Operating Stacks: 1, 2, 3, 4
Unit: 1
Stacks Height (ft): 27.5
Load: 100%

Location (see figure 8)		C ppm	C/C_s (P) x 10,000
RBW	1	1	0
	2	1	0
	3		
	4		
	5		
	6		
RBE	1	66	17
	2	121	32
	3		
	4		
RD		0	0
TBW		0	0
TBE		12	3
AD		14	4
CR		0	0
DGW		3	1
DGE	1	1	0
	2	1	0

TABLE 6 (CONTINUED)

54

Run: 170
Wind Direction (°): 247
Ref. Wind Speed (mph): 21
Operating Stacks: 1, 2, 3, 4
Unit: 1
Stacks Height (ft): 27.5
Load: 100%

Location (see figure 8)		C ppm	C/C_s (P) x 10,000
RBW	1	1	0
	2	1	0
	3		
	4		
	5		
	6		
RBE	1	58	15
	2	131	35
	3		
	4		
RD		1	0
TBW		0	0
TBE		14	4
AD		17	4
CR		1	0
DGW		3	1
DGE	1	1	0
	2	1	0

55

Run: 160
Wind Direction (°): 300
Ref. Wind Speed (mph): 22.5
Operating Stacks: 1, 2, 3, 4
Unit: 1
Stacks Height (ft): 27.5
Load: 100%

Location (see figure 8)		C ppm	C/C_s (P) x 10,000
RBW	1	117	31
	2	186	49
	3		
	4		
	5		
	6		
RBE	1	144	38
	2	126	33
	3		
	4		
RD		0	0
TBW		0	0
TBE		53	14
AD		45	12
CR		0	0
DGW		12	3
DGE	1	36	10
	2	80	21

56

Run: 161
Wind Direction (°): 300
Ref. Wind Speed (mph): 21.3
Operating Stacks: 1
Unit: 1
Stacks Height (ft): 27.5
Load: 100%

Location (see figure 8)		C ppm	C/C_s (P) x 10,000
RBW	1	43	11
	2	64	17
	3		
	4		
	5		
	6		
RBE	1	72	19
	2	69	18
	3		
	4		
RD		0	0
TBW		0	0
TBE		32	8
AD		26	7
CR		1	0
DGW		5	2
DGE	1	23	6
	2	35	9

TABLE 6 (CONTINUED)

57

Run: 125
Wind Direction (°): 180
Ref. Wind Speed (mph): 7
Operating Stacks: 1, 2, 3, 4
Unit: 1
Stacks Height (ft): 46
Load: Idle

Location (see figure 8)		C ppm	C/C_s (P) x 10,000
RBW	1	2	0
	2	3	1
	3		
	4		
	5		
	6		
RBE	1	1	0
	2	0	0
	3		
	4		
RD		0	0
TBW		2	0
TBE		0	0
AD		0	0
CR		4	1
DGW		0	0
DGE	1	0	0
	2		

58

Run: 124
Wind Direction (°): 180
Ref. Wind Speed (mph): 10
Operating Stacks: 1, 2, 3, 4
Unit: 1
Stacks Height (ft): 46
Load: Idle

Location (see figure 8)		C ppm	C/C_s (P) x 10,000
RBW	1	23	6
	2	19	5
	3		
	4		
	5		
	6		
RBE	1	0	0
	2	0	0
	3		
	4		
RD		1	0
TBW		3	1
TBE		0	0
AD		0	0
CR		19	4
DGW		1	0
DGE	1	0	0
	2		

59

Run: 123
Wind Direction (°): 180
Ref. Wind Speed (mph): 13.8
Operating Stacks: 1, 2, 3, 4
Unit: 1
Stacks Height (ft): 46
Load: Idle

Location (see figure 8)		C ppm	C/C_s (P) x 10,000
RBW	1	261	78
	2	235	70
	3		
	4		
	5		
	6		
RBE	1	15	5
	2	6	1
	3		
	4		
RD		5	1
TBW		14	4
TBE		1	0
AD		1	0
CR		18	5
DGW		8	2
DGE	1	3	1
	2		

TABLE 6 (CONTINUED)

60

Run: 122
Wind Direction (°): 180
Ref. Wind Speed (mph): 17
Operating Stacks: 1, 2, 3, 4
Unit: 1
Stacks Height (ft): 46
Load: Idle

Location (see figure 8)		C ppm	C/C_s (P) x 10,000
RBW	1	539	161
	2	563	169
	3		
	4		
	5		
	6		
RBE	1	98	29
	2	50	15
	3		
	4		
RD		28	8
TBW		56	17
TBE		8	3
AD		6	1
CR		24	7
DGW		20	6
DGE	1	20	6
	2		

61

Run: 121
Wind Direction (°): 180
Ref. Wind Speed (mph): 21
Operating Stacks: 1, 2, 3, 4
Unit: 1
Stacks Height (ft): 46
Load: Idle

Location (see figure 8)		C ppm	C/C_s (P) x 10,000
RBW	1	446	133
	2	379	114
	3		
	4		
	5		
	6		
RBE	1	73	22
	2	46	14
	3		
	4		
RD		51	15
TBW		73	22
TBE		10	3
AD		9	3
CR		21	6
DGW		18	5
DGE	1	37	11
	2		

62

Run: 120
Wind Direction (°): 180
Ref. Wind Speed (mph): 25.6
Operating Stacks: 1, 2, 3, 4
Unit: 1
Stacks Height (ft): 46
Load: Idle

Location (see figure 8)		C ppm	C/C_s (P) x 10,000
RBW	1	255	76
	2	210	63
	3	195	58
	4	253	76
	5	283	85
	6	244	73
RBE	1	37	11
	2	16	5
	3	12	4
	4	22	6
RD		58	18
TBW		91	27
TBE		6	1
AD		6	1
CR		17	5
DGW		12	4
DGE	1	20	6
	2		

TABLE 6 (CONTINUED)

63

Run: 206
Wind Direction (°): 180
Ref. Wind Speed (mph): 8
Operating Stacks: 1, 2, 3, 4
Unit: 1
Stacks Height (ft): 2.5
Load: 100%

Location (see figure 8)		C ppm	C/C_s (P) x 10,000
RBW	1	59	16
	2	64	17
	3		
	4		
	5		
	6		
RBE	1		
	2		
	3		
	4		
RD			
TBW			
TBE			
AD			
CR			
DGW			
DGE	1		
	2		

64

Run: 207
Wind Direction (°): 180
Ref. Wind Speed (mph): 10.3
Operating Stacks: 1, 2, 3, 4
Unit: 1
Stacks Height (ft): 2.5
Load: 100%

Location (see figure 8)		C ppm	C/C_s (P) x 10,000
RBW	1	731	193
	2	568	150
	3		
	4		
	5		
	6		
RBE	1		
	2		
	3		
	4		
RD			
TBW			
TBE			
AD			
CR			
DGW			
DGE	1		
	2		

65

Run: 205
Wind Direction (°): 180
Ref. Wind Speed (mph): 12.2
Operating Stacks: 1, 2, 3, 4
Unit: 1
Stacks Height (ft): 2.5
Load: 100%

Location (see figure 8)		C ppm	C/C_s (P) x 10,000
RBW	1	1058	280
	2	984	260
	3		
	4		
	5		
	6		
RBE	1		
	2		
	3		
	4		
RD			
TBW			
TBE			
AD			
CR			
DGW			
DGE	1		
	2		

TABLE 6 (CONTINUED)

66

Run: 204
Wind Direction (°): 180
Ref. Wind Speed (mph): 14.6
Operating Stacks: 1, 2, 3, 4
Unit: 1
Stacks Height (ft): 2.5
Load: 100%

Location (see figure 8)		C ppm	C/C_s (P) x 10,000
RBW	1	1368	362
	2	1225	324
	3		
	4		
	5		
	6		
RBE	1		
	2		
	3		
	4		
RD			
TBW			
TBE			
AD			
CR			
DGW			
DGE	1		
	2		

67

Run: 203
Wind Direction (°): 180
Ref. Wind Speed (mph): 18
Operating Stacks: 1, 2, 3, 4
Unit: 1
Stacks Height (ft): 2.5
Load: 100%

Location (see figure 8)		C ppm	C/C_s (P) x 10,000
RBW	1	1309	346
	2	1072	284
	3		
	4		
	5		
	6		
RBE	1	176	47
	2		
	3		
	4		
RD		47	12
TBW		138	37
TBE		21	6
AD		21	6
CR		37	10
DGW		35	9
DGE	1	46	12
	2	27	7

68

Run: 195
Wind Direction (°): 202
Ref. Wind Speed (mph): 11.7
Operating Stacks: 1, 2, 3, 4
Unit: 1
Stacks Height (ft): 2.5
Load: 100%

Location (see figure 8)		C ppm	C/C_s (P) x 10,000
RBW	1	806	213
	2	644	170
	3		
	4		
	5		
	6		
RBE	1	45	12
	2	39	10
	3		
	4		
RD		1	0
TBW		1	0
TBE		5	1
AD		3	1
CR		24	6
DGW		22	6
DGE	1	5	1
	2	5	1

TABLE 6 (CONTINUED)

69

Run: 196
Wind Direction (°): 202
Ref. Wind Speed (mph): 18
Operating Stacks: 1, 2, 3, 4
Unit: 1
Stacks Height (ft): 2.5
Load: 100%

Location (see figure 8)		C ppm	C/C_s (P) x 10,000
RBW	1	382	101
	2	725	192
	3		
	4		
	5		
	6		
RBE	1	893	236
	2	695	184
	3		
	4		
RD		3	1
TBW		7	2
TBE		145	38
AD		178	47
CR		50	13
DGW			
DGE	1	17	4
	2	17	4

70

Run: 194
Wind Direction (°): 225
Ref. Wind Speed (mph): 11.7
Operating Stacks: 1, 2, 3, 4
Unit: 1
Stacks Height (ft): 2.5
Load: 100%

Location (see figure 8)		C ppm	C/C_s (P) x 10,000
RBW	1		
	2	103	27
	3		
	4		
	5		
	6		
RBE	1	125	33
	2	73	19
	3		
	4		
RD			
TBW			
TBE		4	1
AD		4	1
CR			
DGW			
DGE	1		
	2	4	1

71

Run: 193
Wind Direction (°): 225
Ref. Wind Speed (mph): 15
Operating Stacks: 1, 2, 3, 4
Unit: 1
Stacks Height (ft): 2.5
Load: 100%

Location (see figure 8)		C ppm	C/C_s (P) x 10,000
RBW	1	1	0
	2	4	1
	3		
	4		
	5		
	6		
RBE	1	870	230
	2	760	201
	3		
	4		
RD			
TBW			
TBE		27	7
AD		37	10
CR		1	0
DGW		21	6
DGE	1	5	1
	2		

TABLE 6 (CONTINUED)

72

Run: 192
Wind Direction (°): 225
Ref. Wind Speed (mph): 18
Operating Stacks: 1, 2, 3, 4
Unit: 1
Stacks Height (ft): 2.5
Load: 100%

Location (see figure 8)		C ppm	C/C_s (P) x 10,000
RBW	1	3	1
	2		
	3		
	4		
	5		
	6		
RBE	1	781	207
	2	760	201
	3		
	4		
RD		0	0
TBW		0	0
TBE		100	26
AD		134	35
CR		1	0
DGW		0	0
DGE	1	10	3
	2	10	3

73

Run: 181
Wind Direction (°): 225
Ref. Wind Speed (mph): 21
Operating Stacks: 1, 2, 3, 4
Unit: 1
Stacks Height (ft): 2.5
Load: 100%

Location (see figure 8)		C ppm	C/C_s (P) x 10,000
RBW	1	0	0
	2	24	6
	3		
	4		
	5		
	6		
RBE	1	767	203
	2	700	185
	3		
	4		
RD		0	0
TBW		0	0
TBE		100	26
AD		133	35
CR		1	0
DGW		17	4
DGE	1	7	2
	2	8	2

74

Run: 168
Wind Direction (°): 247
Ref. Wind Speed (mph): 21
Operating Stacks: 1, 2, 3, 4
Unit: 1
Stacks Height (ft): 2.5
Load: 100%

Location (see figure 8)		C ppm	C/C_s (P) x 10,000
RBW	1	0	0
	2	0	0
	3		
	4		
	5		
	6		
RBE	1	238	63
	2	349	92
	3		
	4		
RD		0	0
TBW		0	0
TBE		40	11
AD		50	13
CR		0	0
DGW		10	3
DGE	1	32	8
	2	18	5

TABLE 6 (CONTINUED)

75

Run: 167
Wind Direction (°): 270
Ref. Wind Speed (mph): 21.5
Operating Stacks: 1, 2, 3, 4
Unit: 1
Stacks Height (ft): 2.5
Load: 100%

Location (see figure 8)		C ppm	C/C_s (P) x 10,000
RBW	1	0	0
	2	1	0
	3		
	4		
	5		
	6		
RBE	1	53	14
	2	92	24
	3		
	4		
RD		0	0
TBW		0	0
TBE		33	9
AD		32	8
CR		0	0
DGW		3	1
DGE	1	34	9
	2		

76

Run: 165
Wind Direction (°): 292
Ref. Wind Speed (mph): 21.5
Operating Stacks: 1, 2, 3, 4
Unit: 1
Stacks Height (ft): 2.5
Load: 100%

Location (see figure 8)		C ppm	C/C_s (P) x 10,000
RBW	1	82	22
	2	225	60
	3		
	4		
	5		
	6		
RBE	1	367	97
	2	313	83
	3		
	4		
RD		0	0
TBW		0	0
TBE		127	34
AD		91	24
CR		0	0
DGW		12	3
DGE	1	123	33
	2	94	25

77

Run: 163
Wind Direction (°): 300
Ref. Wind Speed (mph): 22.5
Operating Stacks: 1, 2, 3, 4
Unit: 1
Stacks Height (ft): 2.5
Load: 100%

Location (see figure 8)		C ppm	C/C_s (P) x 10,000
RBW	1	190	50
	2	331	88
	3		
	4		
	5		
	6		
RBE	1	255	67
	2	233	62
	3		
	4		
RD		0	0
TBW		0	0
TBE		90	24
AD		82	22
CR		0	0
DGW		23	6
DGE	1	88	23
	2	95	25

TABLE 6 (CONTINUED)

78

Run: 156
Wind Direction (°): 315
Ref. Wind Speed (mph): 11
Operating Stacks: 1, 2, 3, 4
Unit: 1
Stacks Height (ft): 2.5
Load: 100%

Location (see figure 8)		C ppm	C/C_s (P) x 10,000
RBW	1	22	6
	2	56	15
	3		
	4		
	5		
	6		
RBE	1	36	10
	2	31	8
	3	36	10
	4		
RD		0	0
TBW		0	0
TBE		15	4
AD		13	3
CR		9	2
DGW		2	1
DGE	1	18	5
	2	27	7

79

Run: 155
Wind Direction (°): 315
Ref. Wind Speed (mph): 16
Operating Stacks: 1, 2, 3, 4
Unit: 1
Stacks Height (ft): 2.5
Load: 100%

Location (see figure 8)		C ppm	C/C_s (P) x 10,000
RBW	1	92	24
	2	84	22
	3		
	4		
	5		
	6		
RBE	1	83	22
	2	78	21
	3		
	4		
RD		0	0
TBW		0	0
TBE		40	11
AD		35	9
CR		0	0
DGW		18	5
DGE	1	49	13
	2	87	23

80

Run: 154
Wind Direction (°): 315
Ref. Wind Speed (mph): 21
Operating Stacks: 1, 2, 3, 4
Unit: 1
Stacks Height (ft): 2.5
Load: 100%

Location (see figure 8)		C ppm	C/C_s (P) x 10,000
RBW	1	128	34
	2	112	30
	3		
	4		
	5		
	6		
RBE	1	110	29
	2	106	28
	3		
	4		
RD		1	0
TBW		0	0
TBE		50	13
AD		49	13
CR		0	0
DGW		23	6
DGE	1	56	15
	2	111	30

TABLE 6 (CONTINUED)

81

Run: 153
Wind Direction (°): 337
Ref. Wind Speed (mph): 21.5
Operating Stacks: 1, 2, 3, 4
Unit: 1
Stacks Height (ft): 2.5
Load: 100%

Location (see figure 8)		C ppm	C/C_s (P) x 10,000
RBW	1	77	20
	2	65	17
	3		
	4		
	5		
	6		
RBE	1	63	17
	2	57	15
	3		
	4		
RD		0	0
TBW		0	0
TBE		33	9
AD		33	9
CR		0	0
DGW		19	5
DGE	1	29	8
	1	55	15

82

Run: 152
Wind Direction (°): 360
Ref. Wind Speed (mph): 16
Operating Stacks: 1, 2, 3, 4
Unit: 1
Stacks Height (ft): 2.5
Load: 100%

Location (see figure 8)		C ppm	C/C_s (P) x 10,000
RBW	1	379	100
	2	130	34
	3		
	4		
	5		
	6		
RBE	1	20	5
	2	17	4
	3		
	4		
RD		2	1
TBW		26	7
TBE		2	1
AD		1	0
CR		0	0
DGW		20	5
DGE	1	5	1
	2		

83

Run: 151
Wind Direction (°): 360
Ref. Wind Speed (mph): 21.5
Operating Stacks: 1, 2, 3, 4
Unit: 1
Stacks Height (ft): 2.5
Load: 100%

Location (see figure 8)		C ppm	C/C_s (P) x 10,000
RBW	1	406	107
	2	238	63
	3		
	4		
	5		
	6		
RBE	1	27	7
	2	23	6
	3		
	4		
RD		1	0
TBW		23	6
TBE		6	2
AD		4	1
CR		0	0
DGW		29	8
DGE	1	7	2
	2	0	0

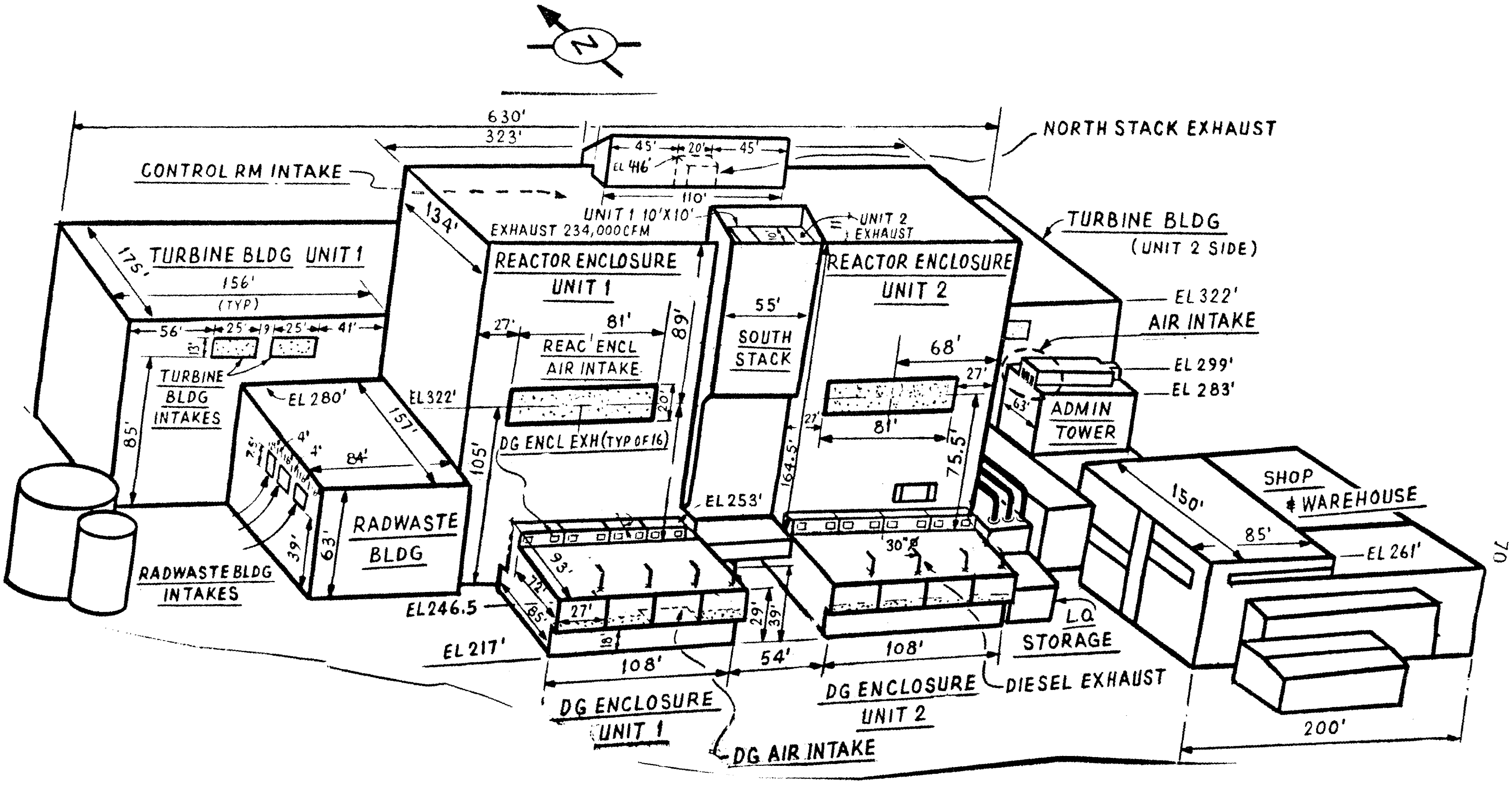

FIGURE 1. SCHEMATIC DESCRIPTION OF THE LGS

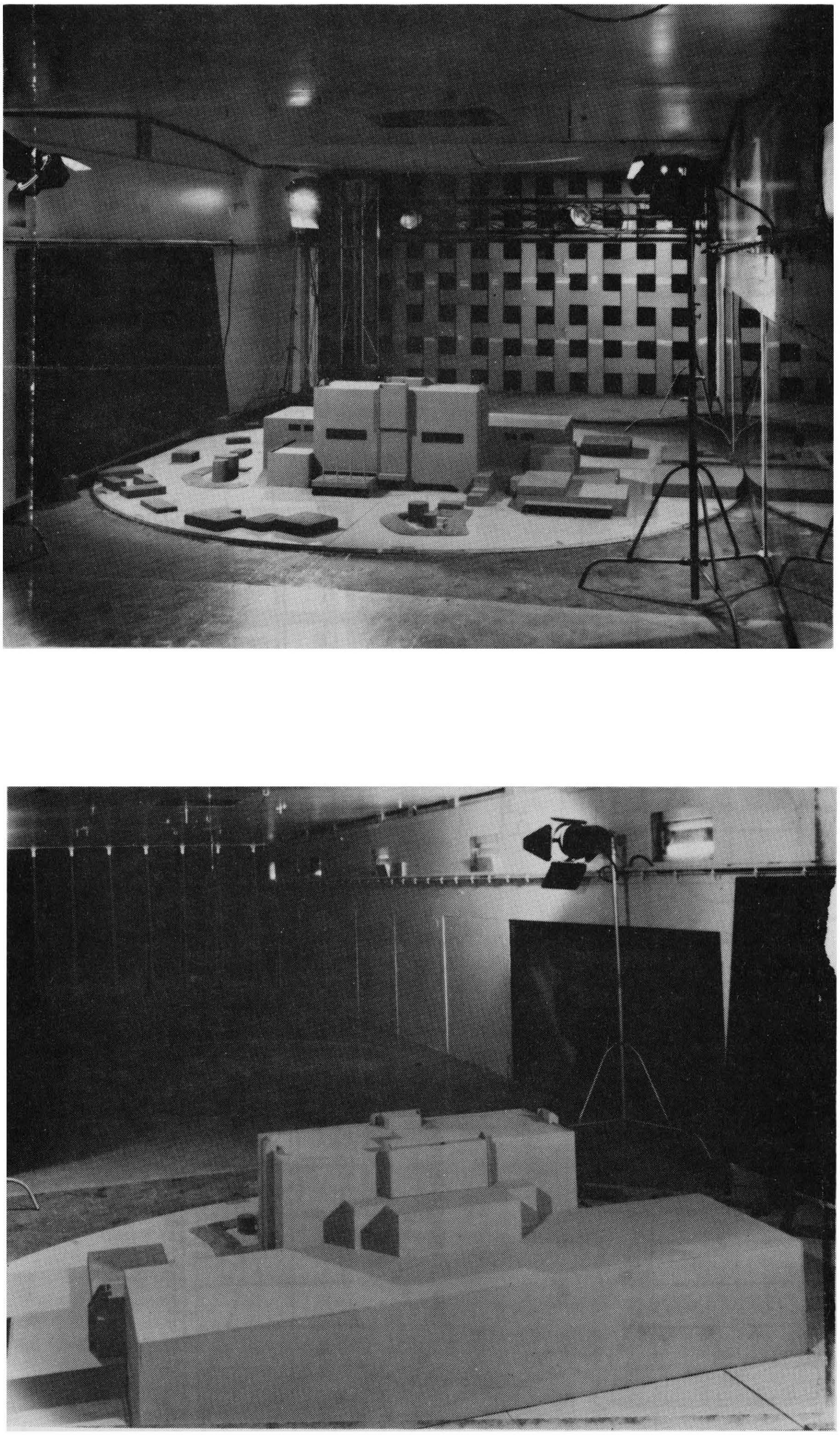

FIGURE 2. THE LGS MODEL IN THE ENVIRONMENTAL WIND TUNNEL

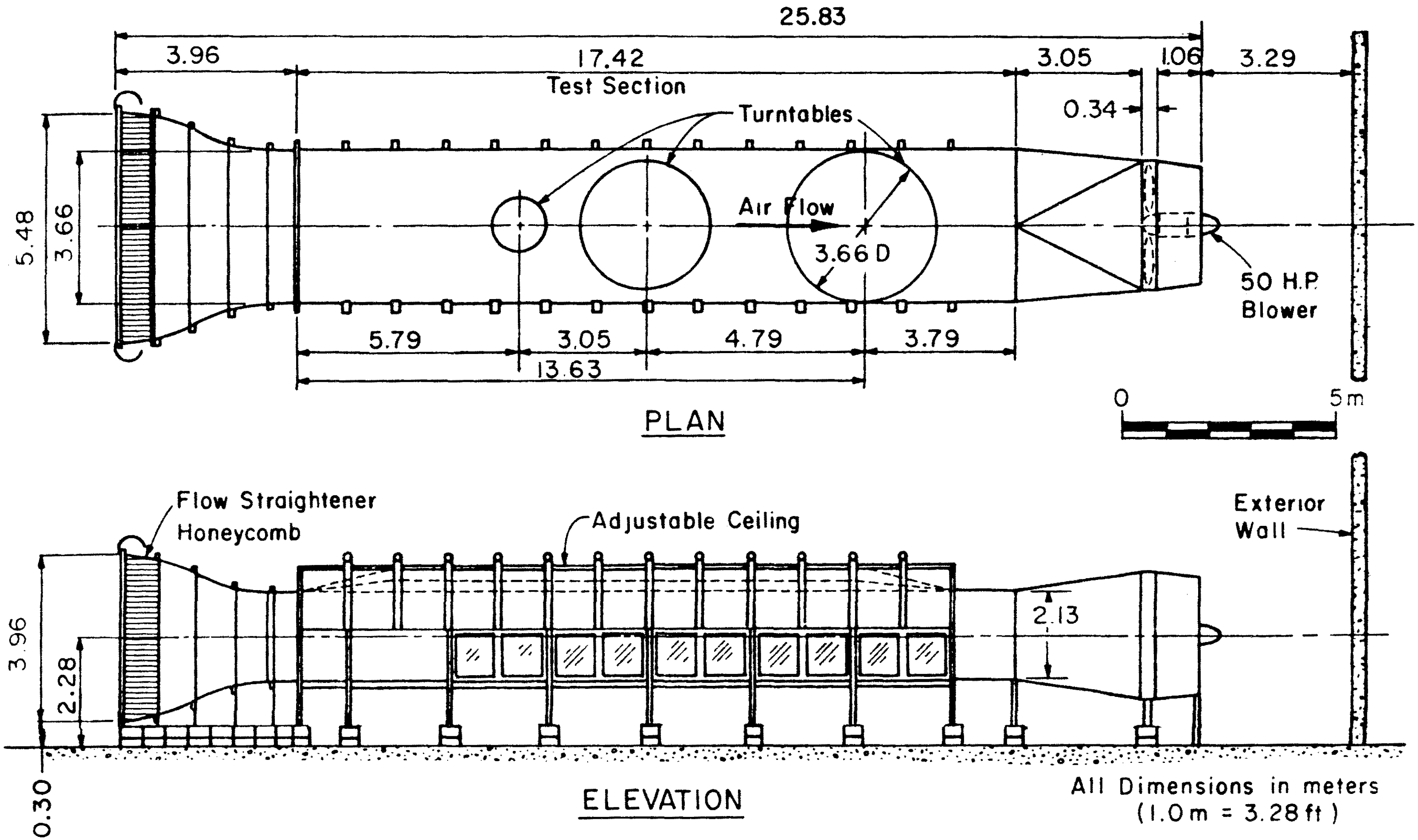

FIGURE 3. ENVIRONMENTAL WIND TUNNEL, FLUID DYNAMICS AND DIFFUSION LABORATORY, COLORADO STATE UNIVERSITY

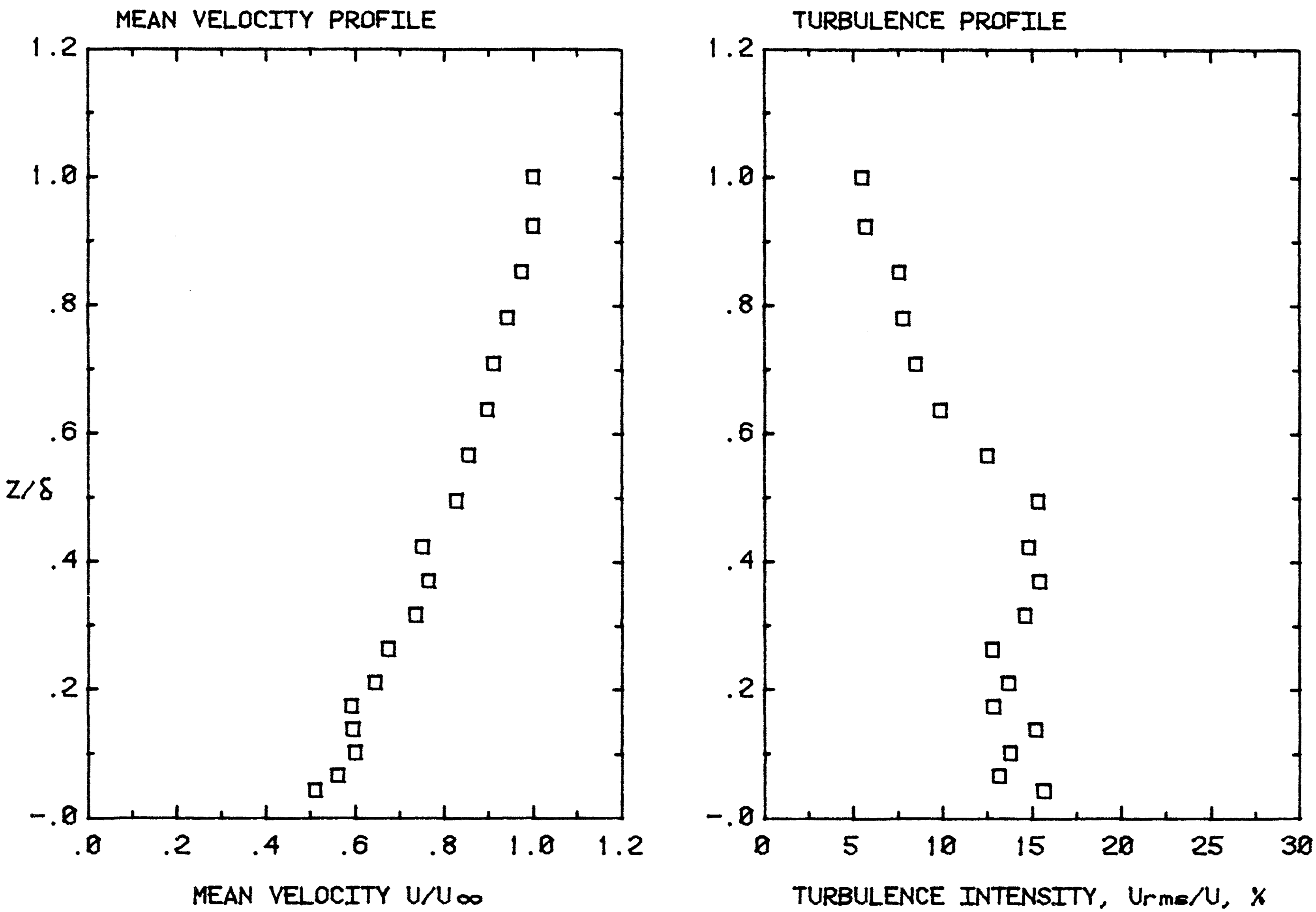

FIGURE 4. MEAN VELOCITY AND TURBULENCE PROFILES APPROACHING THE MODEL

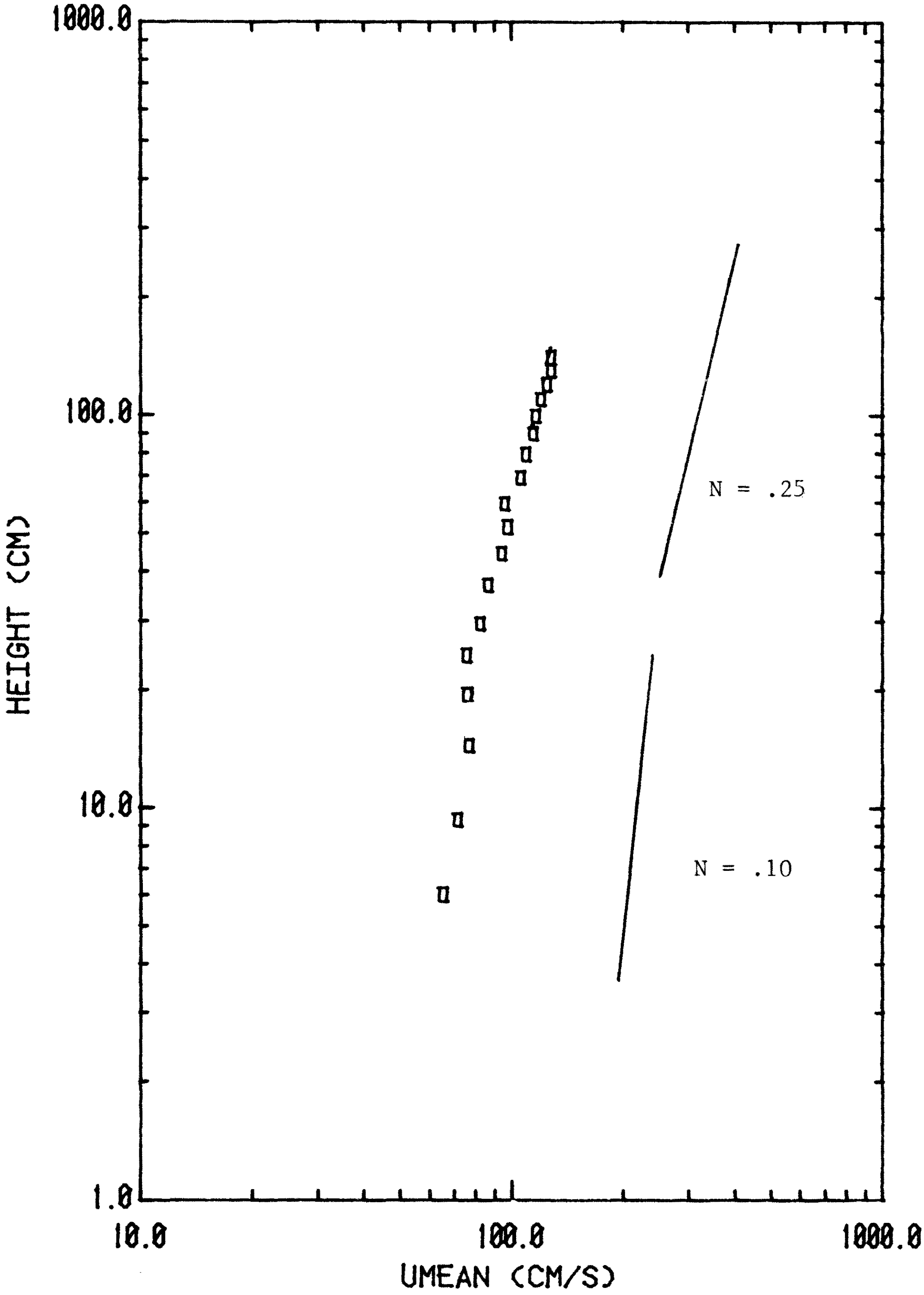

FIGURE 5. LOG-LOG REPRESENTATION OF THE MEAN VELOCITY PROFILE

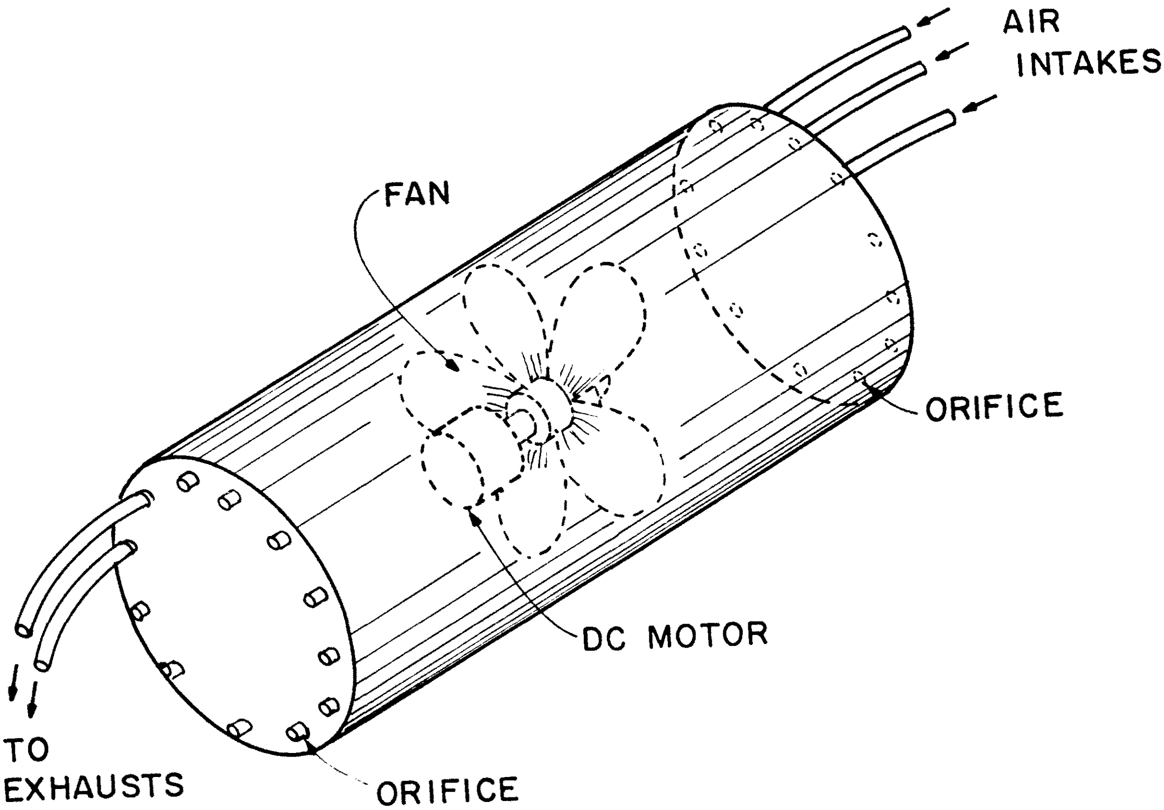

FIGURE 6. SCHEMATIC DESCRIPTION OF THE AIR PUMP FOR THE SIMULATION OF THE VENTILATION SYSTEM

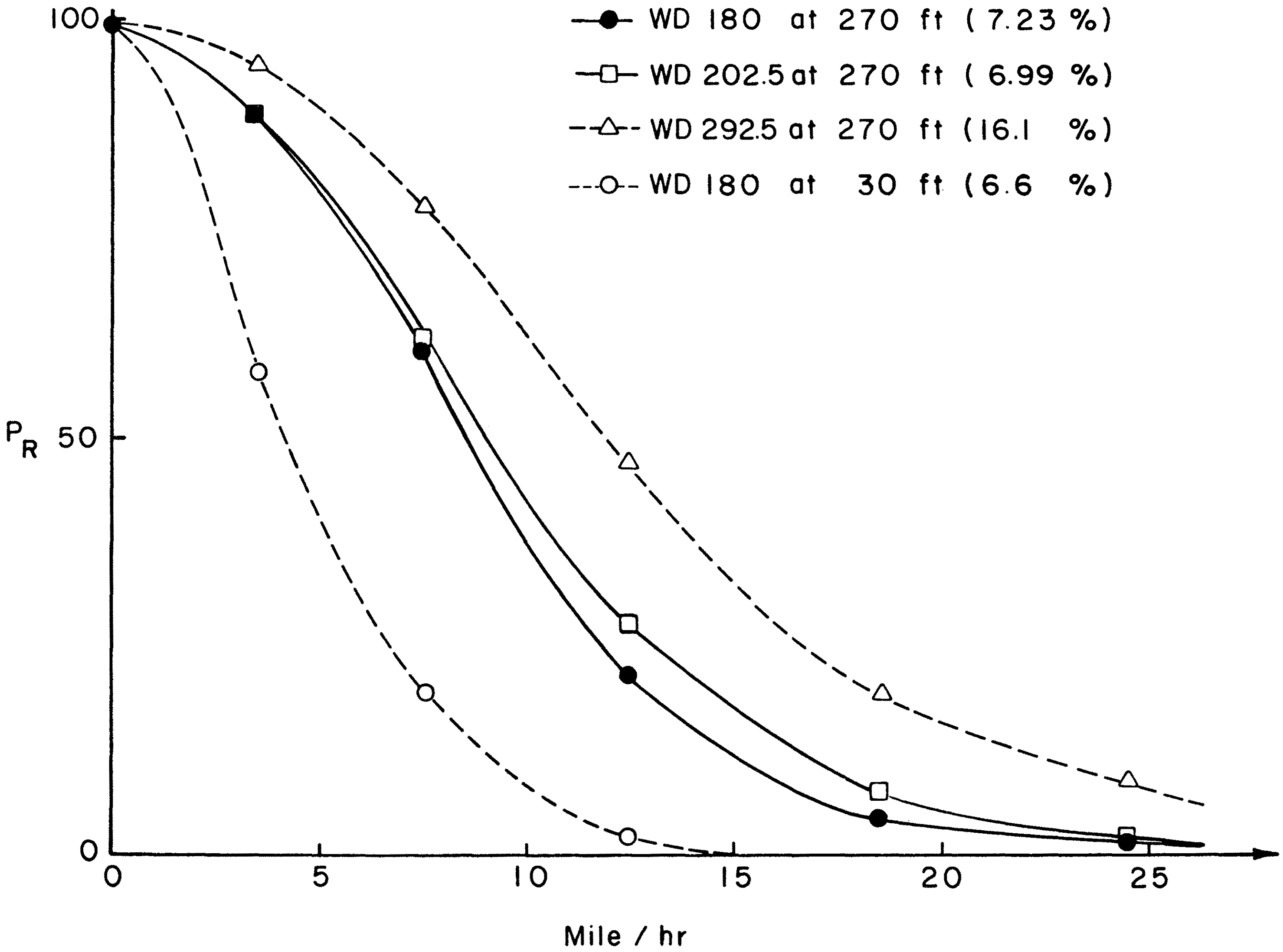

FIGURE 7. PROBABILITIES OF WIND SPEEDS U_T AT THE METEOROLOGICAL TOWER (30 FT) FOR DIFFERENT WIND DIRECTIONS. BASED ON TABLE 3.

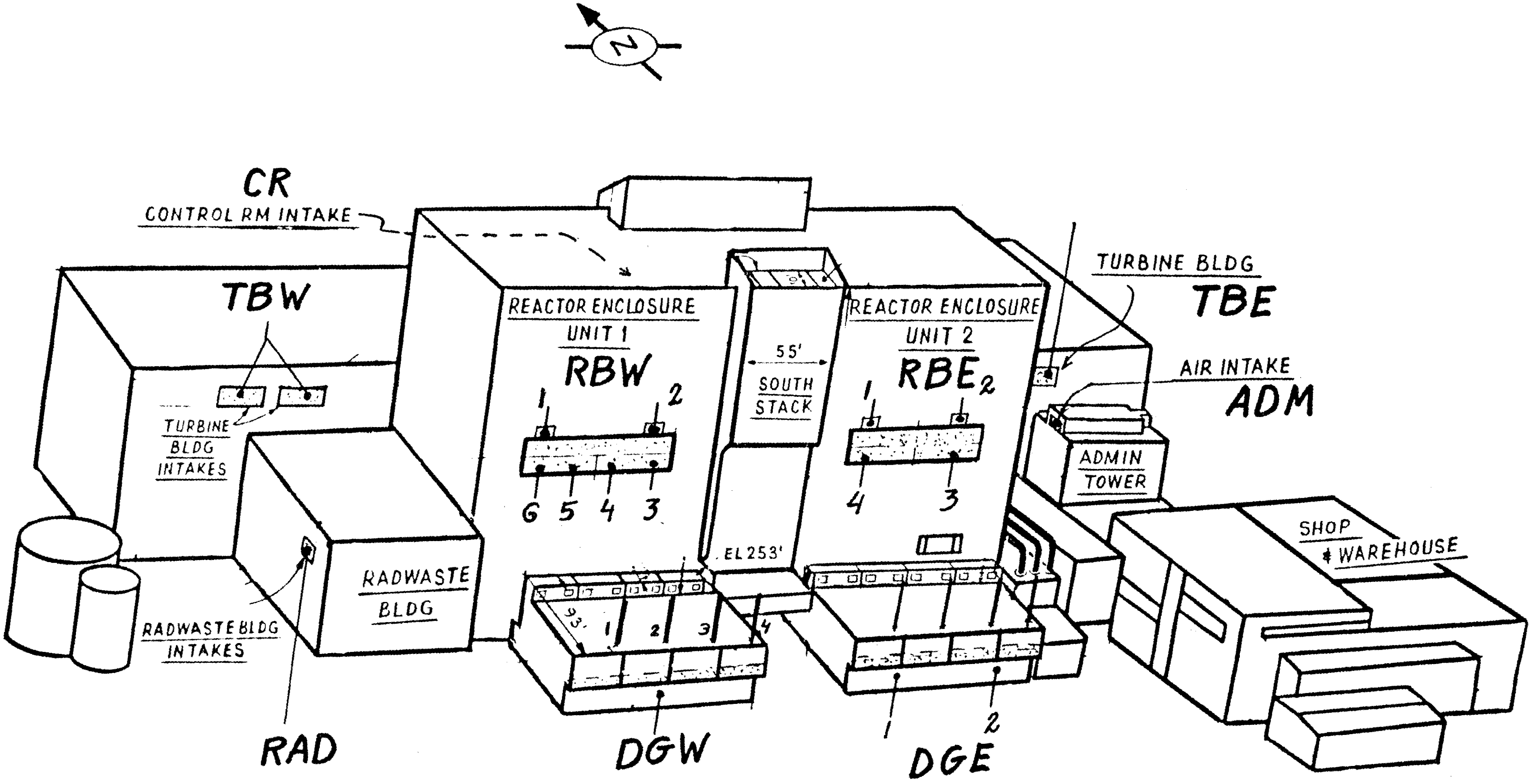

FIGURE 8. LOCATION AND NOTATION OF THE SAMPLING TUBES

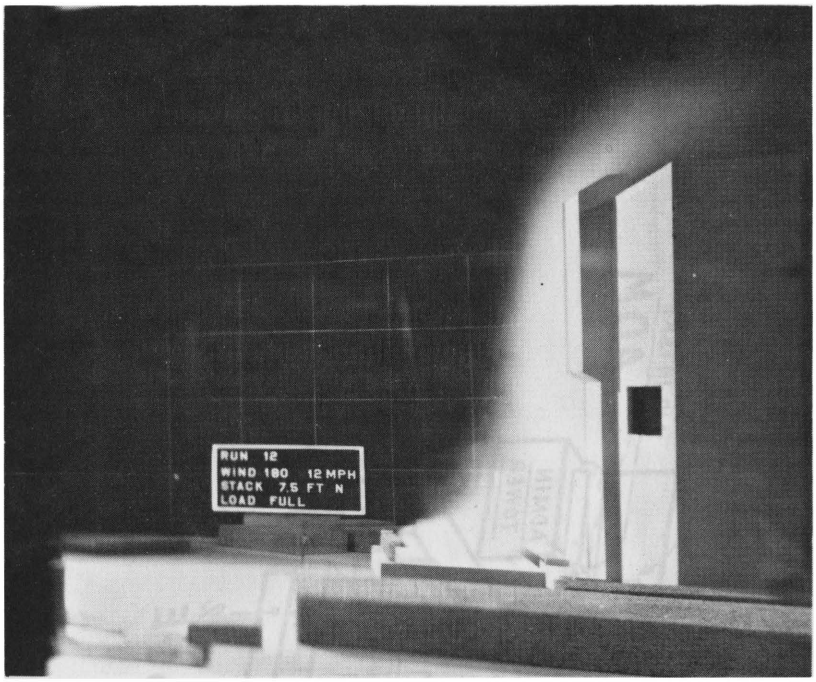

FIGURE 9. FLOW VISUALIZATION OF THE PLUMES FROM THE ORIGINAL STACKS (RUN 12, WD = 180°, U_R = 12 MPH, FULL LOAD)

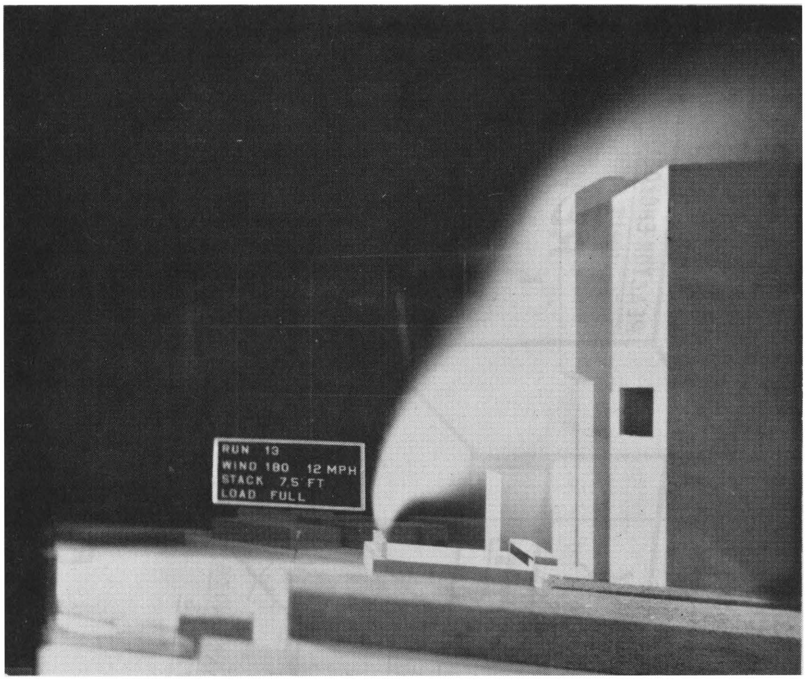

FIGURE 10. FLOW VISUALIZATION OF THE PLUMES FROM 7.5 FT STACKS (RUN 13, WD = 180°, U_R = 12 MPH, FULL LOAD)

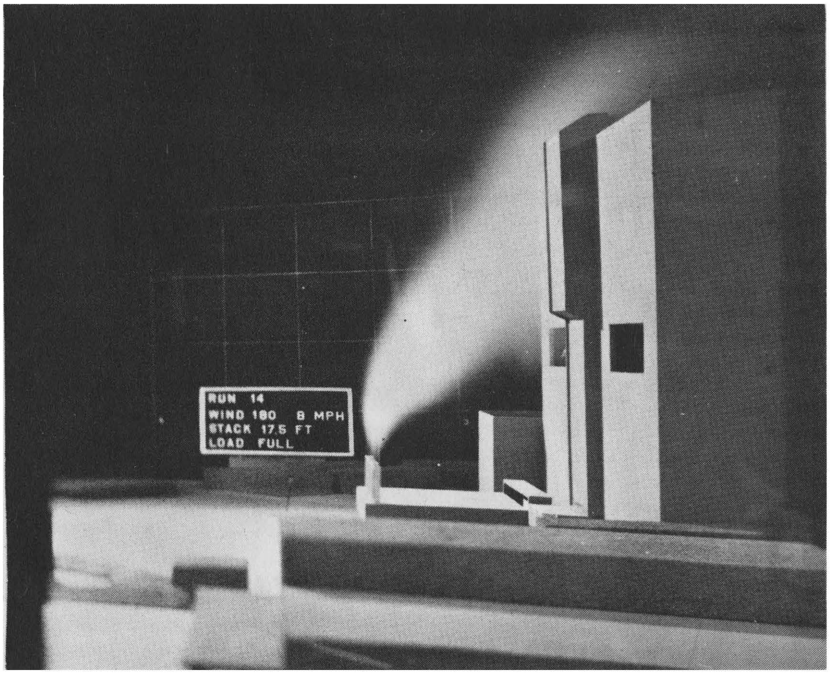

FIGURE 11. FLOW VISUALIZATION OF THE PLUMES FROM 17.5 FT STACKS (RUN 14, WD = 180°, U_R = 8 MPH, FULL LOAD)

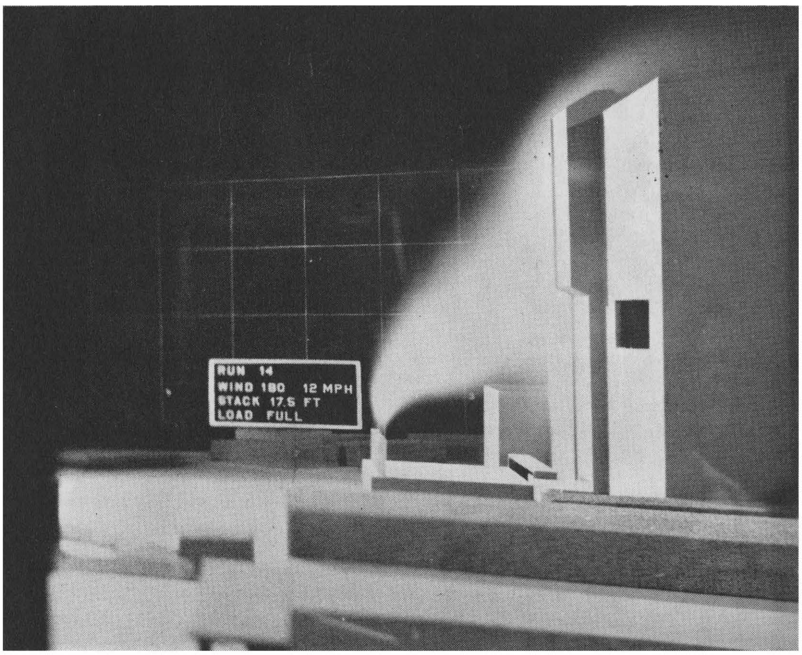

FIGURE 12. FLOW VISUALIZATION OF THE PLUMES FROM 17.5 FT STACKS (RUN 14, WD = 180°, U_R = 12 MPH, FULL LOAD)

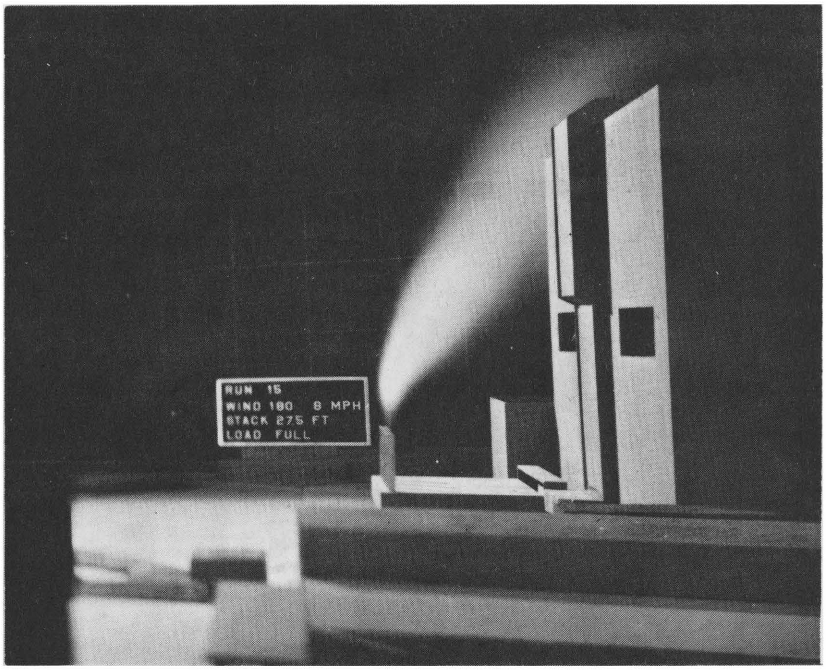

FIGURE 13. FLOW VISUALIZATION OF THE PLUMES FROM 27.5 FT STACKS (RUN 15, WD = 180°, U_R = 8 MPH, FULL LOAD)

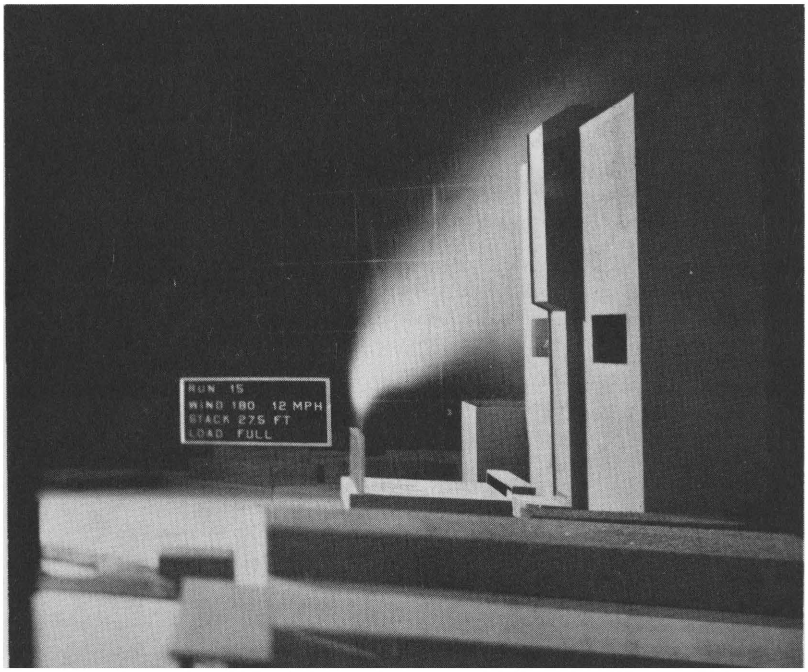

FIGURE 14. FLOW VISUALIZATION OF THE PLUMES FROM 27.5 FT STACKS (RUN 15, WD = 180°, U_R = 12 MPH, FULL LOAD)

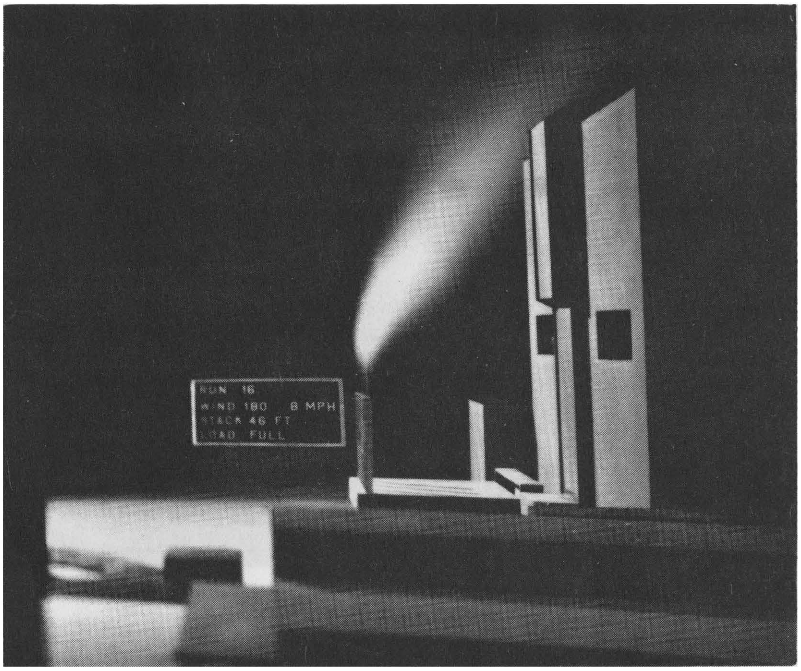

FIGURE 15. FLOW VISUALIZATION OF THE PLUMES FROM 46 FT STACKS (RUN 16, WD = 180°, U_R = 8 MPH, FULL LOAD)

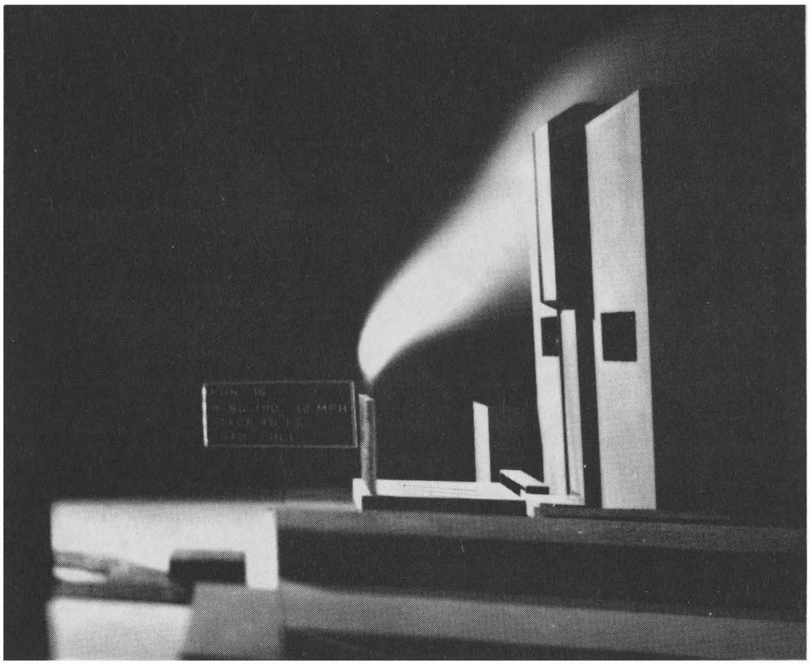

FIGURE 16. FLOW VISUALIZATION OF THE PLUMES FROM 46 FT STACKS (RUN 16, WD = 180°, U_R = 12 MPH, FULL LOAD)

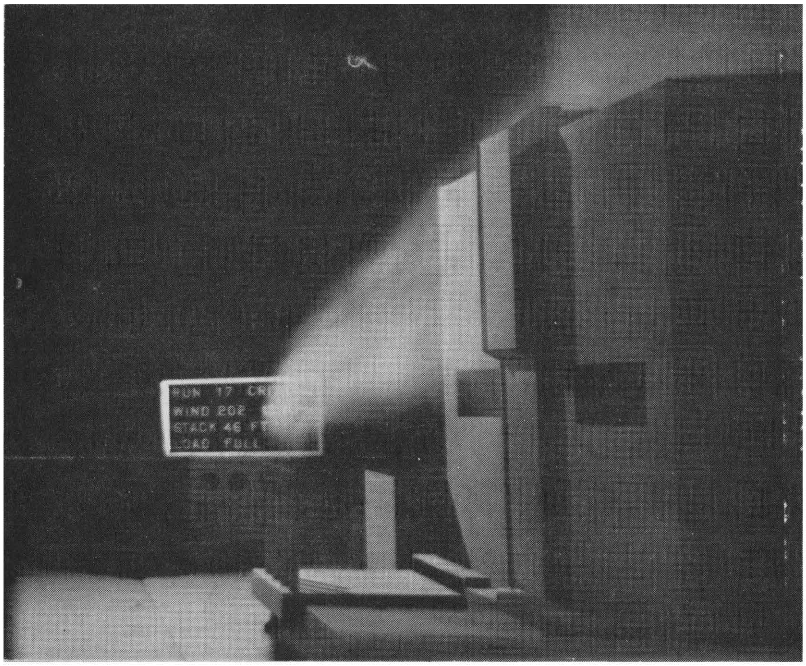

FIGURE 17. FLOW VISUALIZATION OF THE PLUMES FROM 46 FT STACKS (RUN 17, WD = 202°, U_R = 16 MPH, FULL LOAD)

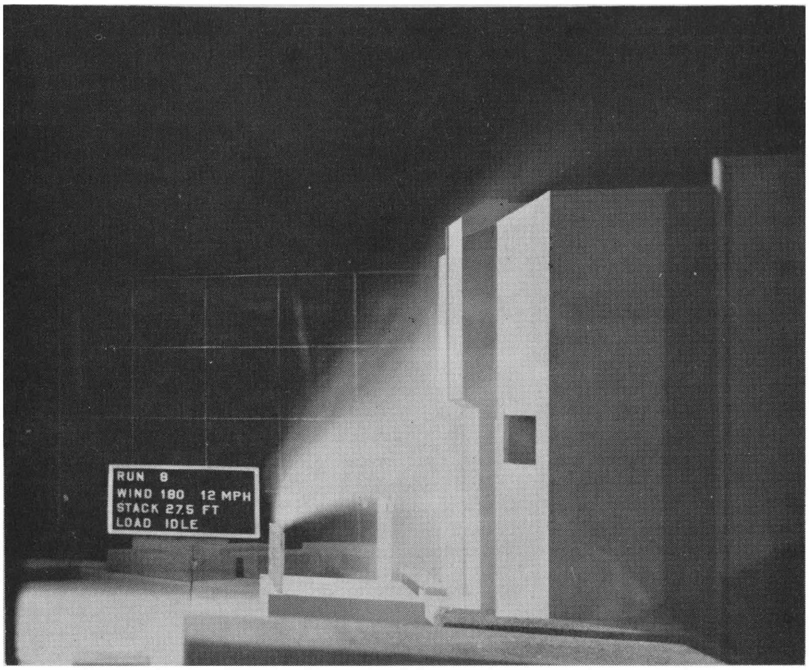

FIGURE 18. FLOW VISUALIZATION OF THE PLUMES FROM 27.5 FT STACKS (RUN 8, WD = 180°, U_R = 12 MPH, IDLE LOAD)

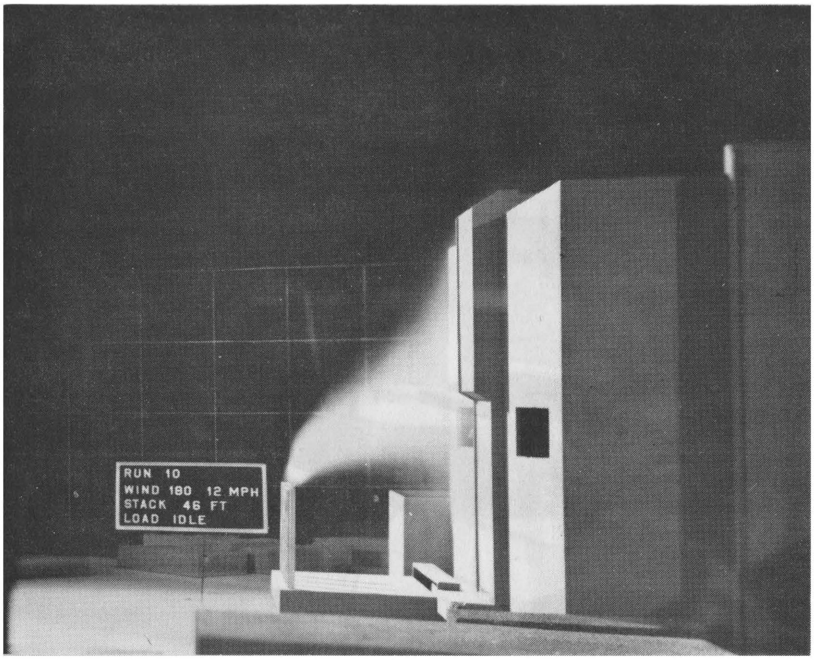

FIGURE 19. FLOW VISUALIZATION OF THE PLUMES FROM 46 FT STACKS (RUN 10, WD = 202°, U_R = 12 MPH, IDLE LOAD)

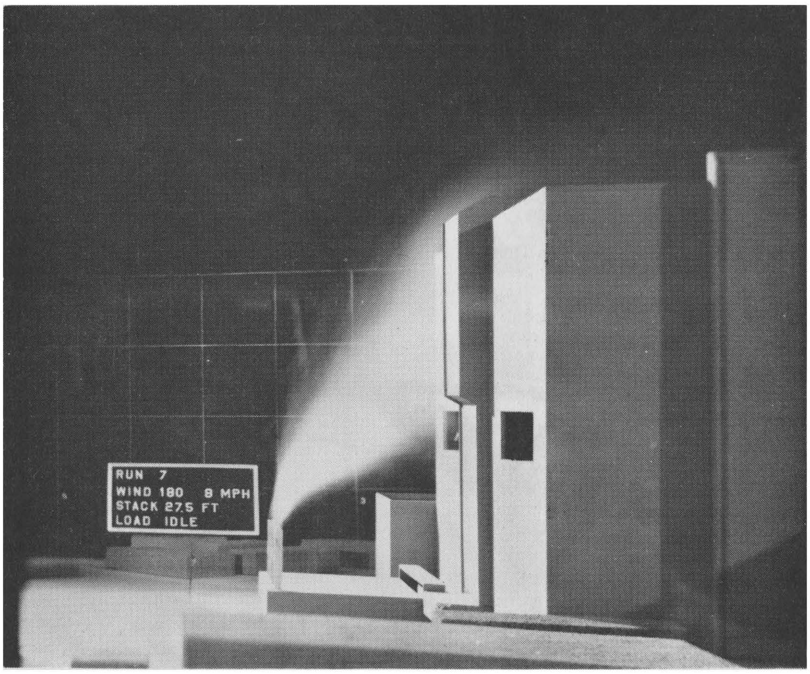

FIGURE 20. FLOW VISUALIZATION OF THE PLUMES FROM 27.5 FT STACKS (RUN 7, WD = 180°, U_R = 8 MPH, IDLE LOAD)

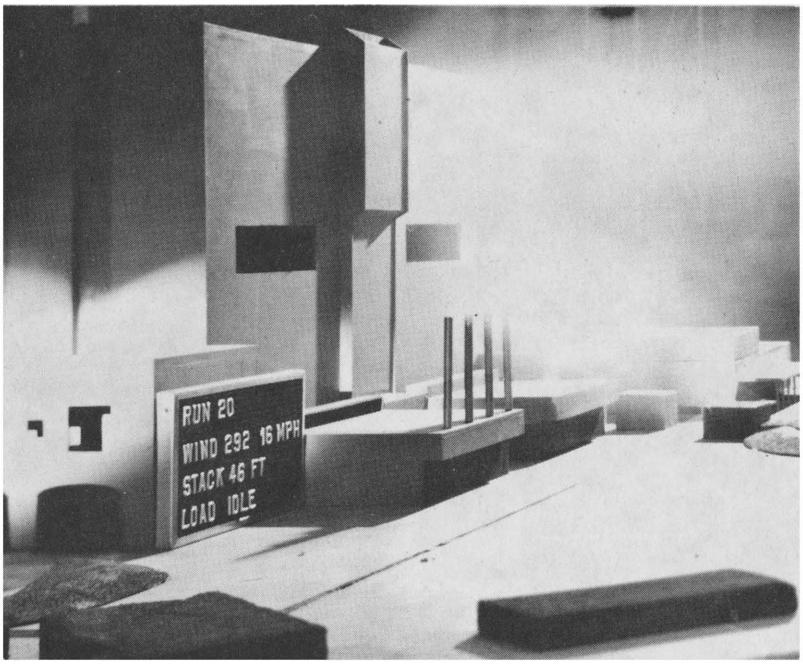

FIGURE 21. FLOW VISUALIZATION OF THE PLUMES FROM 46 FT STACKS (RUN 20, WD = 292°, U_R = 16 MPH, IDLE LOAD)

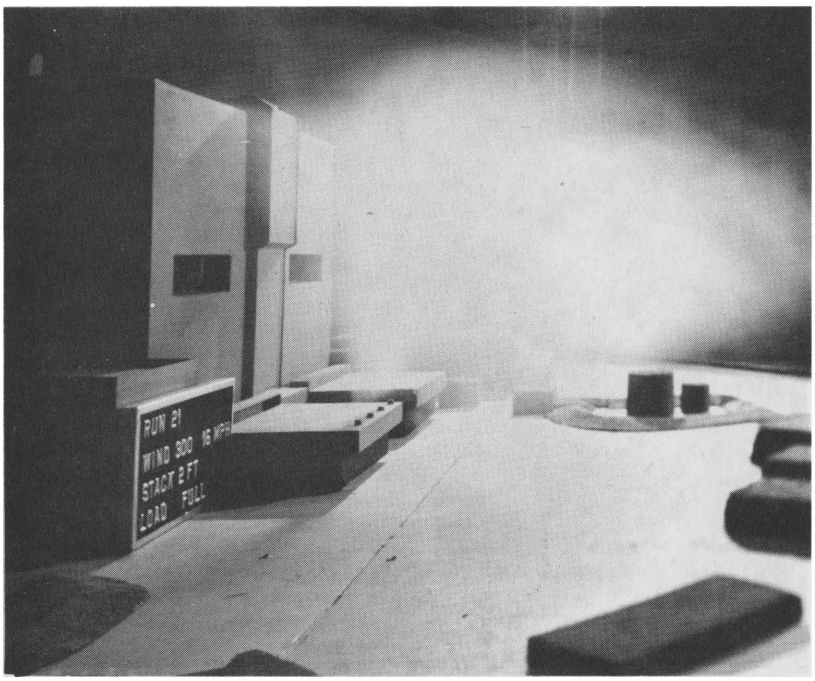

FIGURE 22. FLOW VISUALIZATION OF THE PLUMES FROM 2 FT STACKS (RUN 21, WD = 300°, U_R = 16 MPH, FULL LOAD)

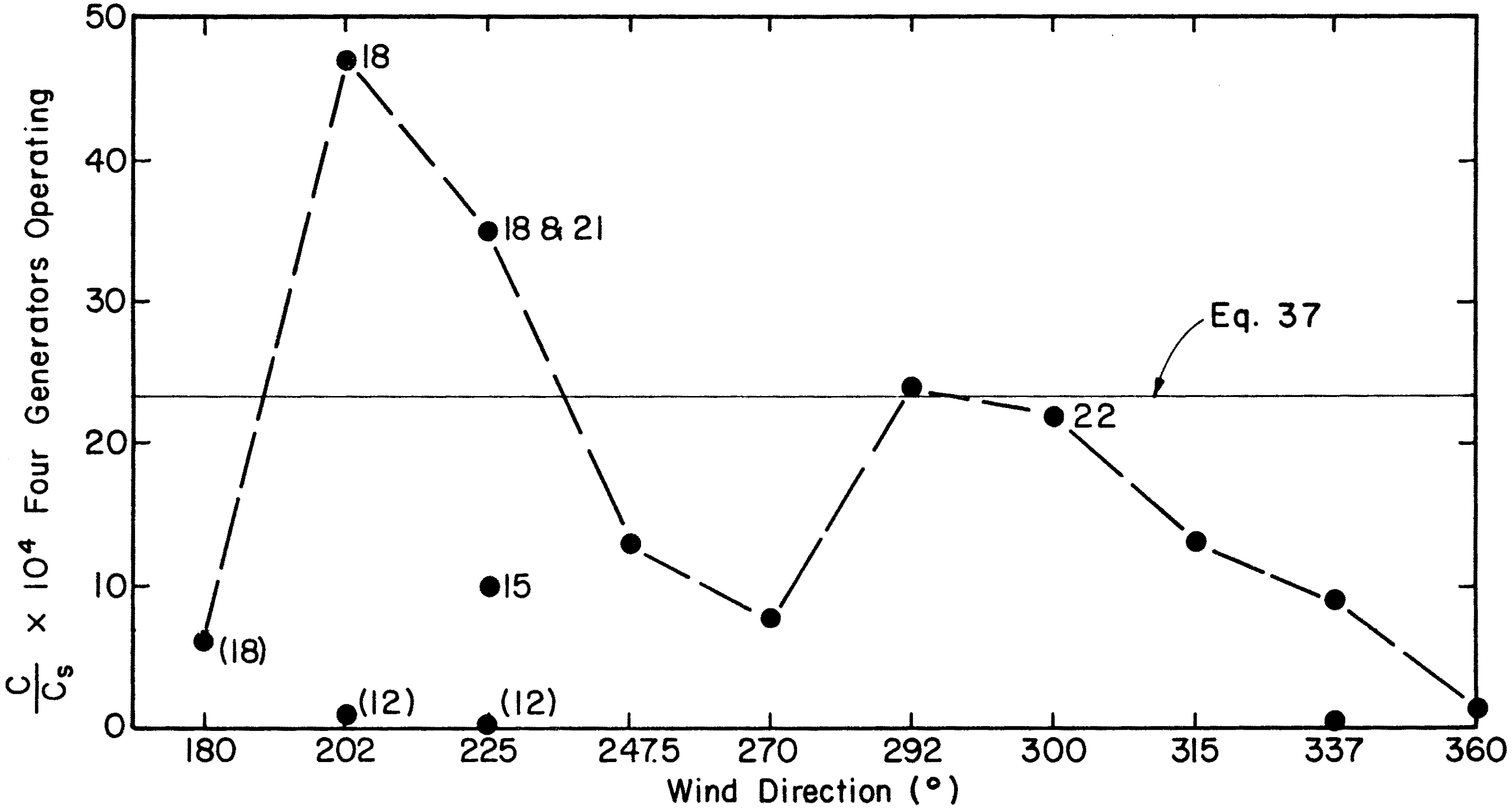

FIGURE 23. CONCENTRATION RATIOS AT THE ADMINISTRATION BUILDING DURING OPERATION OF FOUR DIESEL GENERATORS (FULL LOAD) WITH 2.5 FT STACKS. (WIND SPEED U_R = 21 MPH EXCEPT WHEN OTHERWISE NOTED NEAR DATA POINT.)

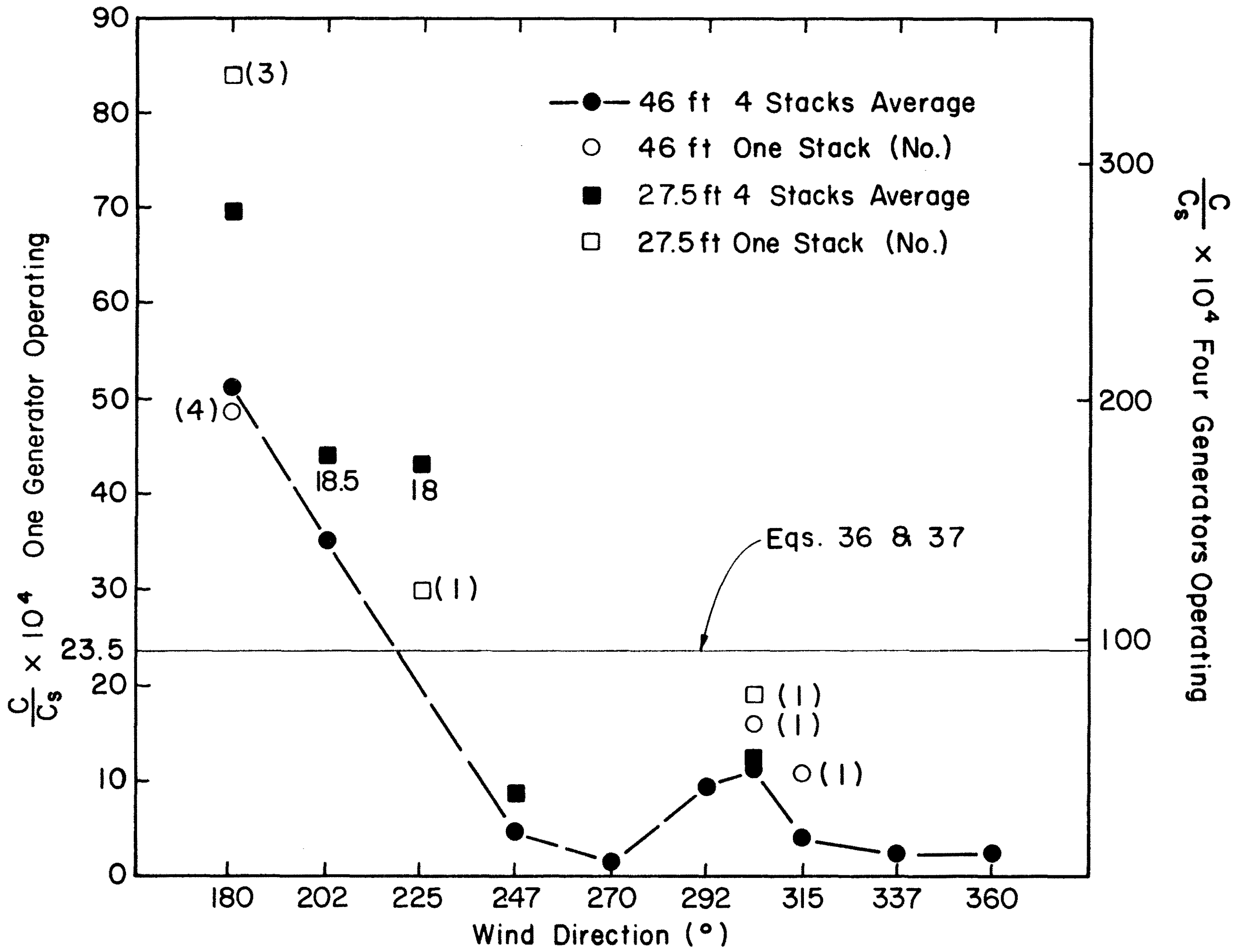

FIGURE 24. MAXIMUM CONCENTRATION RATIOS AT THE REACTOR BUILDING AIR INTAKES AT HIGH WIND SPEEDS FOR DIFFERENT WIND DIRECTIONS (FULL LOAD)

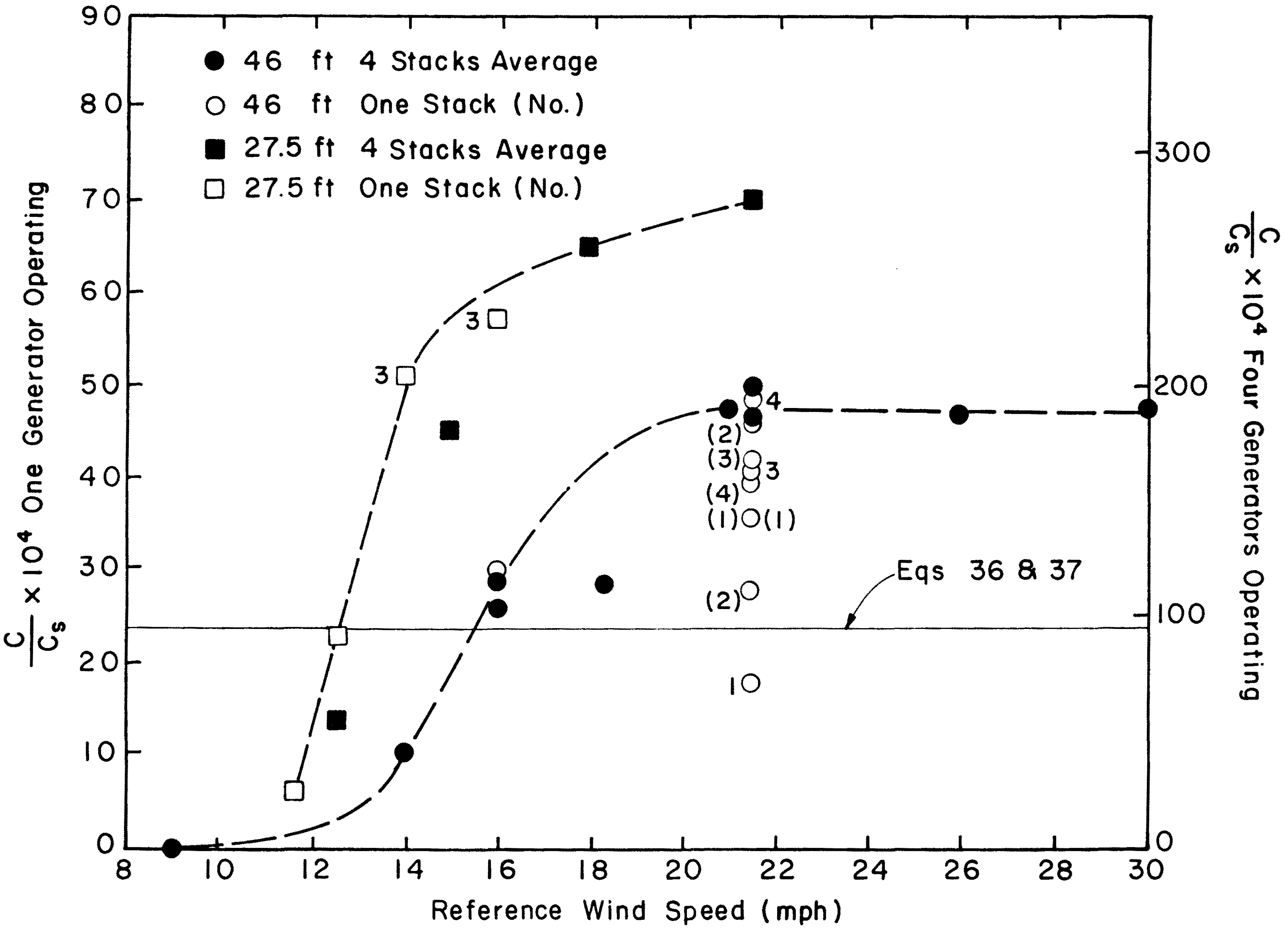

FIGURE 25. MAXIMUM CONCENTRATION RATIOS AT RBW FOR WD = 180°, AT DIFFERENT WIND SPEEDS (FULL LOAD)

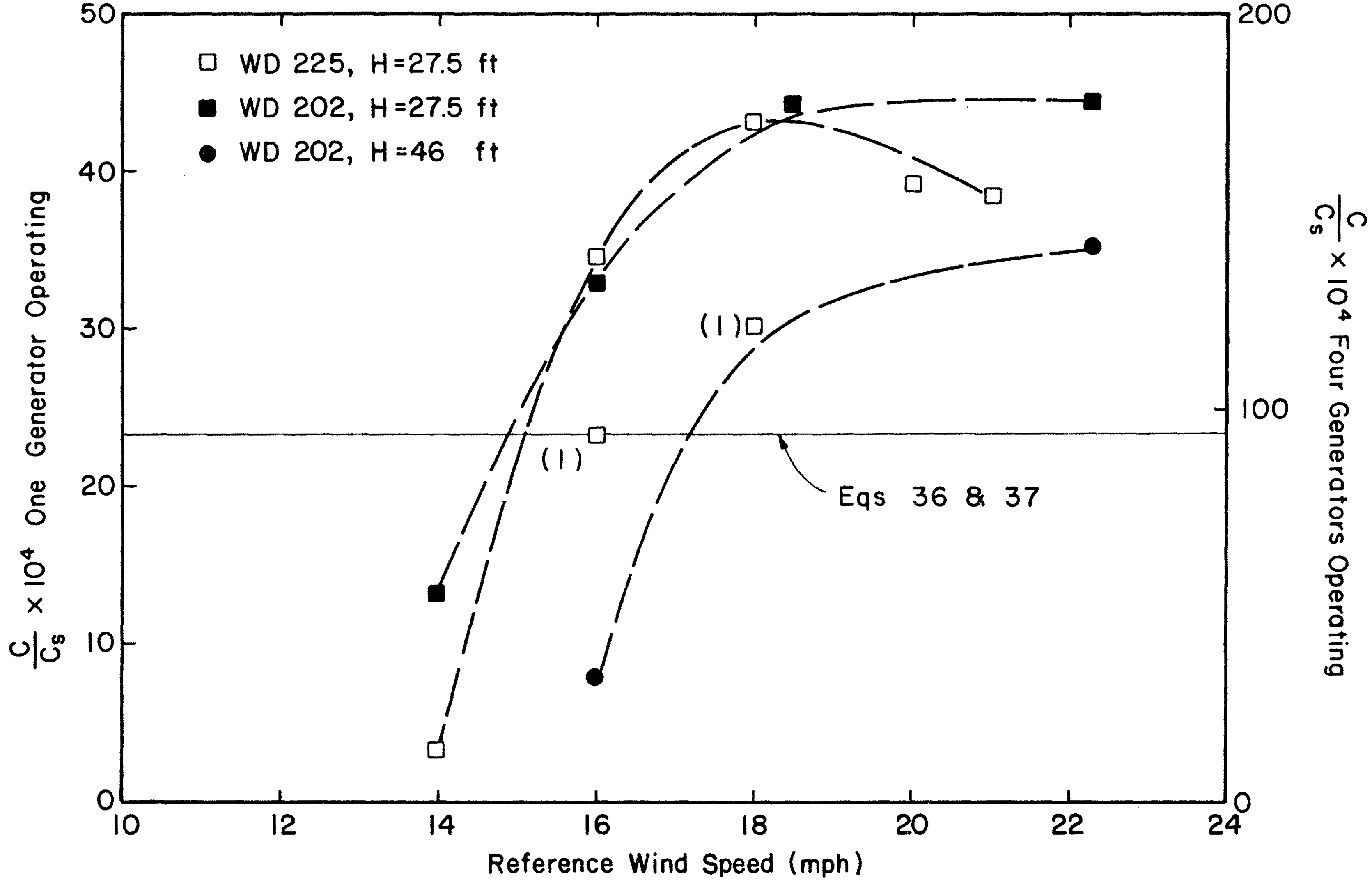

FIGURE 26. MAXIMUM CONCENTRATION RATIOS FOR WD = 202° AND 225° AT DIFFERENT WIND SPEEDS (FULL LOAD)

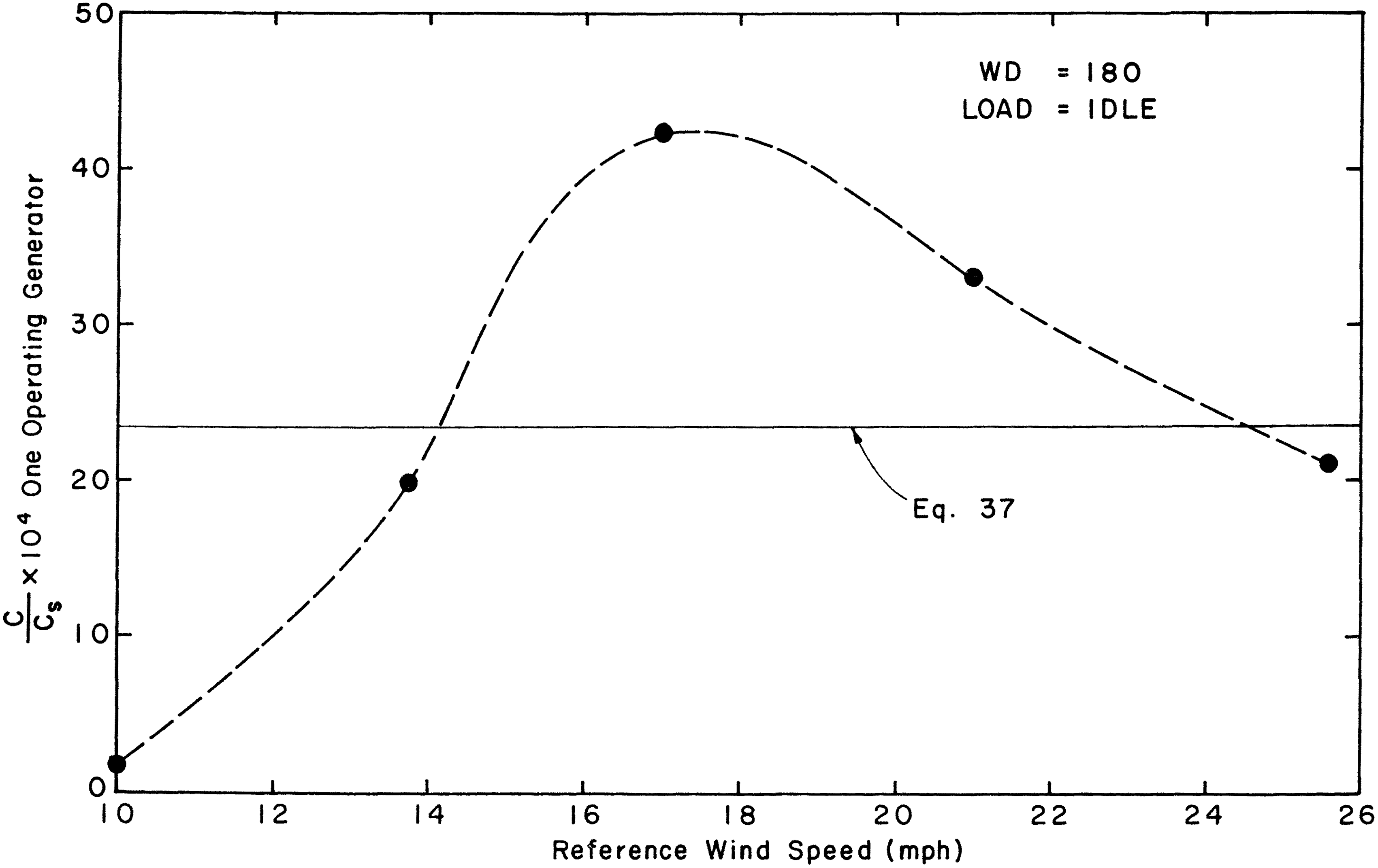

FIGURE 27. MAXIMUM CONCENTRATION RATIOS FOR WD = 180° AT DIFFERENT WIND SPEEDS (H = 46 FT, IDLE LOAD)

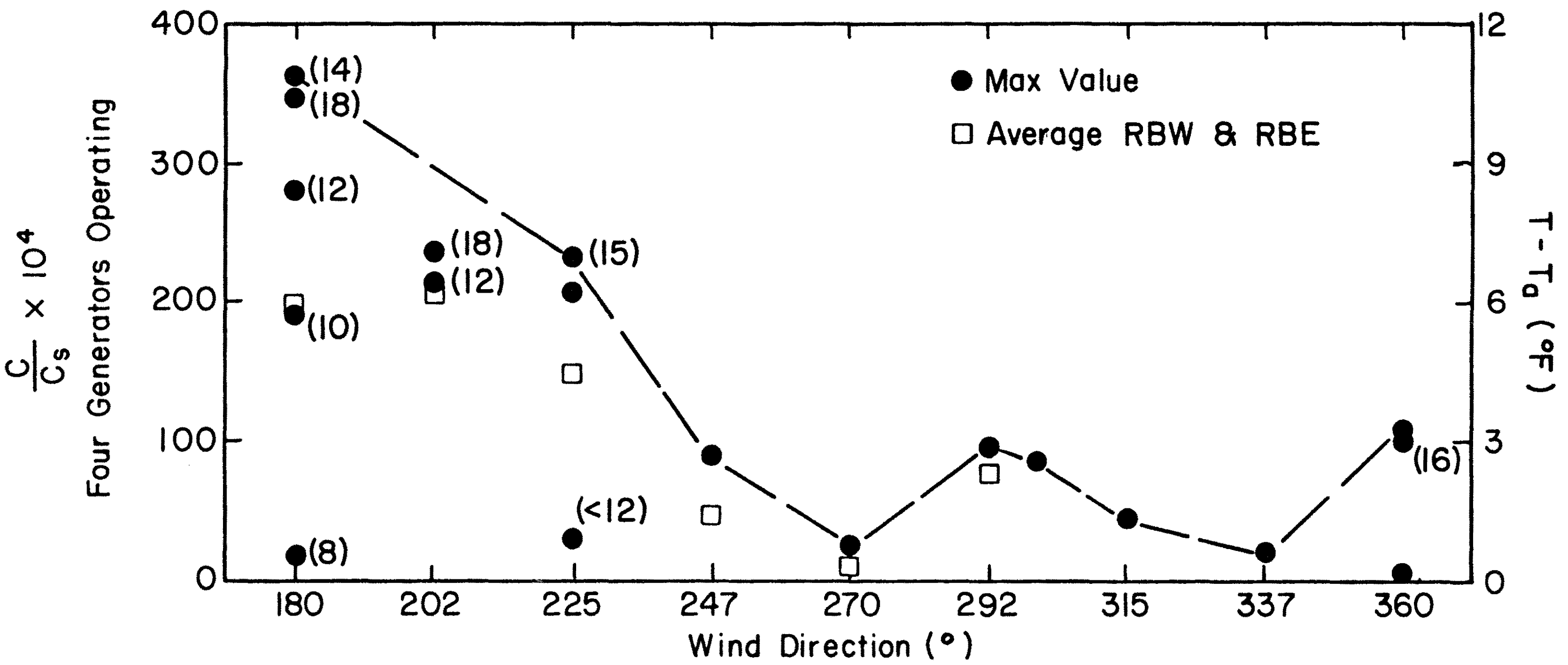

FIGURE 28. MAXIMUM CONCENTRATION RATIO AT THE REACTOR ENCLOSURE BUILDING AIR INTAKES DURING OPERATION OF FOUR DIESEL GENERATORS WITH 2.5 FT STACK (WIND SPEED 21 MPH EXCEPT WHEN OTHERWISE NOTED NEAR DATA POINTS).